https://doi.org/10.5194/egusphere-2026-3657
Preprint. Discussion started: 27 July 2026

Physical-Biogeochemical Coupling in the Baltic Sea: How Joint Assimilation of Chlorophyll-a and SST Reshapes Thermal Structure and Ecosystem Representation

Ye Liu[1] and WeiWei Fu[2]

[1]Department of Research and Development, Swedish Meteorological and Hydrological Institute, Norrköping, Sweden
[2]Department of Atmospheric and Oceanic Sciences, Fudan University, Shanghai, China

Correspondence to: Ye Liu (ye.liu@smhi.se)

Abstract. The coupled physical–biogeochemical dynamics of the Baltic Sea are challenging to simulate due to its complex bathymetry, strong stratification, and high optical turbidity. This study evaluates a multi-source data assimilation framework using a three-dimensional coupled model, comparing univariable (chlorophyll-a only) and multivariable (chlorophyll-a plus sea surface temperature) assimilation strategies. Our results quantify the vertical and dynamical limits of surface-constrained assimilation in stratified marginal seas. Satellite chlorophyll-a assimilation markedly improves the spatial and seasonal representation of surface phytoplankton biomass, but in situ profiles are necessary to accurately reconstruct the subsurface chlorophyll maximum. Physical and biological constraints are complementary, and their joint assimilation yields a synergistic improvement, substantially reducing thermohaline biases and enhancing overall model consistency. Although chlorophyll-a increases can modify subsurface heating through bio-optical feedback, deep-water oxygen profiles at monitoring stations remain insensitive to surface-focused constraints and are governed instead by physical ventilation and remineralization. Crucially, the joint configuration provides a cross-variable regularization that prevents noisy biological updates from degrading the physical state. These results demonstrate that, in optically complex marginal seas, joint physical–biogeochemical assimilation is essential to overcome the limitations of univariable frameworks and to ensure that surface observations translate into an accurate representation of the full water column.

https://doi.org/10.5194/egusphere-2026-3657
Preprint. Discussion started: 27 July 2026

1. Introduction

The Baltic Sea ranks among the world's most heavily affected marine ecosystems. Its semi-enclosed basin, limited water exchange with the North Sea, low salinity, and strong vertical stratification collectively hinder the dilution and export of land-derived pollutants, rendering the basin exceptionally vulnerable to anthropogenic pressures (Jahanmard, et al., 2025; Liblik et al., 2022). Over recent decades, excessive nitrogen and phosphorus inputs from agricultural and industrial waste have triggered widespread eutrophication, recurrent phytoplankton blooms, and expanding hypoxic zones (Gustafsson et al., 2012; Savchuk, 2018; Andersen et al., 2017), with profound consequences for cycling and ecosystem functioning across the basin (Meier et al., 2022).

Chlorophyll-a (Chl-a), the primary photosynthetic pigment in phytoplankton, serves as a widely used proxy for phytoplankton biomass and a proxy for primary productivity (Siegel et al, 2013, Clow et al., 2026). A realistic characterization of Chl-a variability is therefore essential for assessing ecological status and tracking eutrophication dynamics in coastal seas (Maúre et al., 2021). In the Baltic Sea, both in situ and satellite observations reveal strong spatiotemporal variability in Chl-a, driven by complex interactions among stratification, nutrient availability, freshwater inputs, and light conditions (Carstensen et al, 2020; Brando et al., 2021; Stramska and Jakacki, 2024). However, numerical ecosystem models consistently fail to capture this variability – particularly bloom timing, spatial distribution, and intensity – due to coarse resolution, oversimplified biological parameterizations, poor representation of regional optical properties, and insufficient integration of high-resolution observational data (Neumann et al., 2021; Soomets et al., 2022; Meier et al., 2019; Ruvalcaba Baroni et al., 2024).

In global and regional oceans, data assimilation (DA) has been widely and successfully applied to physical variables (e.g., temperature, salinity, sea surface height) systems, producing substantial improvements in reanalysis and forecast skill (Stammer et al., 2016; Karspeck et al, 2018; Liu et al., 2021; Lai et al, 2021). Assimilation of biogeochemical variables, including nutrients, dissolved oxygen, and occasionally Chl-a, has recently emerged as a promising approach for improving ecosystem model simulations in regional seas (Liu et al, 2014; Ciavatta et al, 2018; Teruzzi et al., 2021). However, most coupled systems treat the physical and biogeochemical update steps independently, and the mechanisms by which biological increments propagate into the physical state – or are dampened by it – remain poorly understood, especially in optically complex, salinity-stratified marginal seas (Goodliff et al., 2019; Skákala et al., 2021). Weakly coupled frameworks, in which physical and biogeochemical variables share a common state vector but are updated without explicit cross-variable error covariances, offer a practical intermediate method. Such frameworks avoid the risk of introducing spurious cross-covariances but still allow the nonlinear model dynamics to mediate indirect physical–biogeochemical interactions during the forecast step. Nevertheless, the effectiveness of this indirect coupling pathway, as well as the conditions under which it fails, have not been systematically assessed for the Baltic Sea.

https://doi.org/10.5194/egusphere-2026-3657
Preprint. Discussion started: 27 July 2026

The Baltic Sea presents a particularly demanding environment for satellite-based chlorophyll-a assimilation. A major difficulty arises from high concentrations of riverine-derived colored dissolved organic matter (CDOM), which dominate light absorption at blue wavelengths throughout the year and contribute more than 80% of total light absorption at 400 nm across large parts of the Baltic Sea (Kratzer and Moore, 2018; Simis et al., 2017). This optical complexity challenges ocean color retrieval algorithms and also compromises atmospheric correction procedures. As a result, satellite-derived Chl-a products in the Baltic Sea exhibit systematic biases, especially in coastal and estuarine eutrophicated zones (Kratzer and Moore, 2018; Tilstone et al., 2022). Recent advances in CDOM-explicit bio-optical modelling (Neumann et al., 2021) and in dedicated regional Chl-a algorithms for Sentinel-3 OLCI have partially mitigated these biases, but assimilation of satellite products still requires preprocessing and robust error characterization to prevent the propagation of retrieval bias into the model state (Lavigne et al., 2021; Brando et al., 2021). Furthermore, the haline stratification that dominates the Baltic vertical structure constrains the coupling between thermal, biological, and physical processes. Unlike thermally stratified open-ocean systems, the buoyancy impact of bio-optical heating anomalies in the Baltic is expected to be modest relative to the stabilizing salinity gradient, fundamentally altering the expected cross-variable responses.

Despite the maturity of coupled biogeochemical modelling of the Baltic Sea including operational reanalysis and forecast systems, the direct assimilation of Chl-a within the Baltic context remains underused. Moreover, to date, no comprehensive studies have yet systematically assessed how the joint assimilation of satellite and in situ Chl-a together with sea surface temperature (SST) influences the simulation of phytoplankton dynamics and physical–biogeochemical feedback within a weakly coupled framework (Ciavatta et al., 2018; Goodliff et al., 2019; Teruzzi et al., 2021). This study addresses this gap using a controlled set of assimilation experiments conducted within the NEMO–SCOBI modelling system, using the LSEIK ensemble filter. We examine how different DA strategies affect the representation of phytoplankton phenology and spatial biomass distribution, as well as coupled physical–biogeochemical interactions in the Baltic Sea. By assimilating high-resolution satellite and in situ Chl-a data, we provide observational constraints for an optically complex marginal sea system. Through this suite of experiments, we quantify the relative and combined effects of Chl-a and SST assimilation on model performance. Specifically, we evaluate: (i) how assimilating satellite and in situ Chl-a, separately and in combination, modifies the representation of phytoplankton phenology and spatial biomass patterns; (ii) how biologically induced variations in light absorption influence upper-ocean thermal structure and stratification within a weakly coupled system; and (iii) how assimilation impact differs across the surface layer, the subsurface chlorophyll maximum (SCM), and the deep oxygen environment, thereby clarifying which components of the vertical water column can be realistically constrained by multi-source assimilation in an optically complex marginal sea. By addressing these questions, the study moves beyond traditional performance assessment toward a process-oriented understanding, establishing a mechanistic basis for assessing both the potential and the limits of joint physical–biogeochemical assimilation in the Baltic Sea and similar CDOM-rich, salinity-stratified coastal systems.

https://doi.org/10.5194/egusphere-2026-3657
Preprint. Discussion started: 27 July 2026

2. Model Configuration and Data

2.1 Model: NEMO-SCOBI

A coupled ocean–biogeochemical modeling system was configured for the Baltic–North Sea based on the NEMO framework (Nucleus for European Modelling of the Ocean), with a horizontal resolution of approximately 3.7 km (2 nautical miles) and 56 vertical levels with variable thickness. Near the surface, layers are finely resolved at about 3 m to capture stratification and upper-layer dynamics, and the maximum layer thickness reaches 22 m in the deepest parts of the basin, such as the Norwegian Trench. Open boundaries to the English Channel and between Scotland and Norway use the Flather radiation condition (Flather, 1994) for depth-integrated (barotropic) velocities and the Flow Relaxation Scheme (Davies, 1976) for relaxing tracer variables (temperature, salinity, and biogeochemical components). The model adopts a nonlinear free surface with a split-explicit time-stepping scheme to separately resolve fast barotropic and slower baroclinic components. Lateral boundaries apply free-slip conditions for momentum, and bottom friction is calculated using a quadratic drag law with spatially varying roughness lengths. Vertical mixing is parameterized using a k–ε turbulence closure scheme (Umlauf and Burchard, 2003), with mixing-length limitation following Galperin et al. (1988) to maintain realistic stratification in strongly stratified regions. Tracer advection is computed using a Total Variation Diminishing (TVD) scheme to ensure numerical stability and conservation (Leclair and Madec, 2009). Isopycnal diffusion is enhanced near river inflows to prevent negative salinity values, especially in areas of intense freshwater discharge such as the Neva estuary.

The biogeochemical processes are simulated in this study by the SCOBI (Swedish Coastal and Ocean Biogeochemical) module, which is online-coupled with NEMO to simulate essential biogeochemical dynamics, including nutrient cycling (nitrate, ammonium, phosphate, silicate), oxygen dynamics, primary and secondary production (phytoplankton and zooplankton), and detritus decomposition (Eilola et al. 2009; Ruvalcaba Baroni et al., 2024). In SCOBI, hydrogen sulfide concentrations are represented by “negative oxygen” equivalents (1 mL H_2S L^{-1} = -2 mL O_2 L^{-1}) (Fonselius, 1962). Biogeochemical tracers are transported by the physical flow and interact through local biogeochemical transformations. The open boundaries for biogeochemical variables are prescribed using monthly climatological fields. Sea ice processes are simulated with the LIM3 model, which accounts for both thermodynamic growth and melt and dynamic sea-ice transport.

The coupled system is initialized from a reanalysis simulation described by von Schuckmann et al. (2019). Atmospheric forcing is provided by the UERRA regional reanalysis with hourly data at 11 km resolution (Ridal et al., 2017; Copernicus Climate Change Service, 2019). A precipitation correction factor of 0.8 is applied to account for known overestimation. At the open boundaries in the North Sea, hydrographic variables and sea level are prescribed using ECMWF’s ORAS4/5 reanalyses (Balmaseda et al., 2013; Zuo et al., 2018), supplemented by barotropic surge levels from the NOAMOD model (She et al., 2007). Freshwater inflow is represented using daily river discharge from the EHYPE hydrological model (Arheimer et al., 2012), with river salinity fixed at 0.001 PSU and temperature matched to the local sea surface temperature.

https://doi.org/10.5194/egusphere-2026-3657
Preprint. Discussion started: 27 July 2026

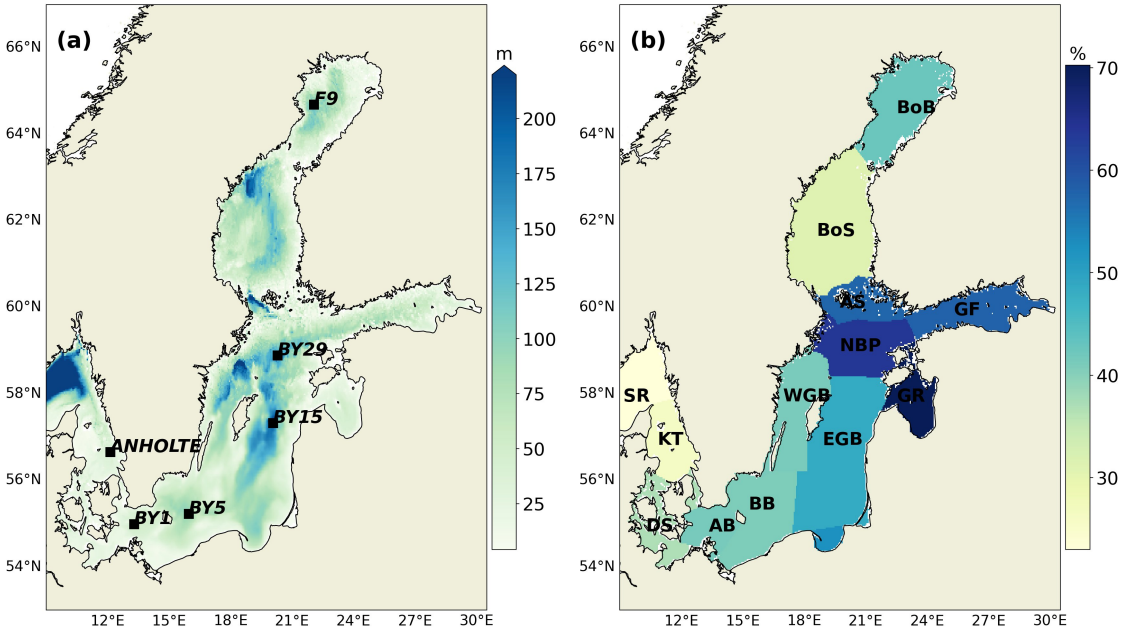

Figure 1. Map of the study area showing the discretized model bathymetry(a). The squares show the locations of the representative in situ monitoring stations. The positions of Baltic sub-basins and correponding relative errors of satellite observations to the in situ observations statisticaled in the basin are shown in figure(b) for Skagerrak (SR), Kattgat (KT), Danish straits (DS), Arokna basin (AB), Bornholm basin (BB), east Gotland basin (EGB), west Gotland basin (WGB), north Baltic proper (NBP), Gulf of Finland (GF), Gulf of Riga (GR), Åland Sea (ÅS), Bothnian Sea (BoS), and Bothnian bay (BoB).

2.2 Observational Datasets

2.2.1 Chlorophyll-a

Two satellite-derived Chl-a datasets from Copernicus Marine Service (CMEMS) product OCEANCOLOUR_BAL_BGC_L3_MY_009_133 were assimilated, differing in spatial resolution and temporal coverage. The first dataset has a 1 km spatial resolution and is a multi-sensor product combining observations from several ocean color instruments (e.g., MODIS, VIIRS, MERIS, SeaWiFS, OLCI–S3A), providing a consistent long-term record. The second dataset offers higher resolution (300 m) and is derived from Sentinel-3 OLCI Level-3 observations within the same processing framework, available from 2016 onwards. Both datasets provide near-daily observations, depending on cloud conditions and orbital cycles, and cover the entire Baltic Sea. Only clear-sky satellite observations were used in the assimilation, and all data were filtered using quality flags to minimize contamination from atmospheric effects and land adjacency.

https://doi.org/10.5194/egusphere-2026-3657
Preprint. Discussion started: 27 July 2026

The combined assimilation of these datasets enhances spatial coverage and representation of variability across scales relative to a single-product approach. Differences in sensor characteristics and resolution result in complementary sampling from basin to coastal scales. Specifically, the 1 km dataset constrains basin-scale variability, while the 300 m dataset captures finer-scale features, particularly in coastal and heterogeneous waters. Their joint use enables consistent representation of large-scale patterns while improving the characterization of small-scale phytoplankton dynamics.

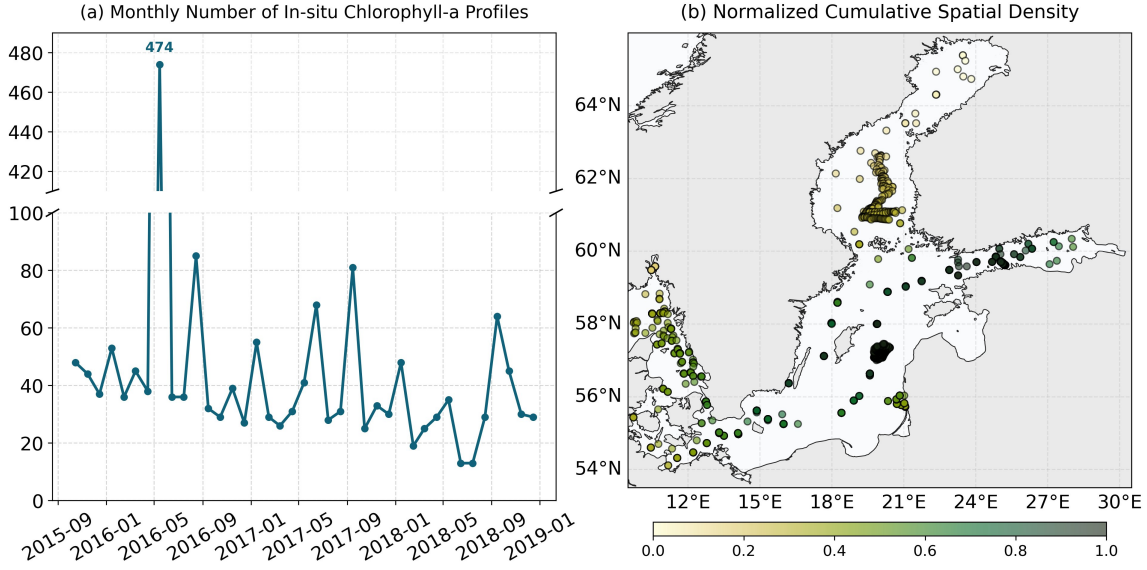

Figure 2. Temporal frequency and normalized spatial density of unique Baltic Sea in situ profiles between October 2015 and December 2018. (a) Monthly sampling sequence showing standard baseline monitoring (13 to 85 profiles/month) punctuated by an extensive high-resolution cruise in May 2016 (474 profiles). (b) Basin-wide spatial sampling density mapping derived via smooth Gaussian kernel density estimation. The color scale highlights the geometric footprint of high-frequency undulating cross-basin transects overlaid on traditional fixed monitoring stations.

In situ Chl-a measurements were obtained from the CMEMS Bio-In Situ Thematic Assembly Centre database (product ID: INSITU_BAL_PHYBGCWAV_DISCRETE_MYNRT_013_032) comprising fluorometric Chl-a observations derived from CTD casts in the Baltic Sea. The database provides observations over an extended nominal period; however, only data corresponding to the period of this study were used. The observations are spatially and temporally heterogeneous, with denser coverage near long-term monitoring stations and during summer survey periods. Vertical sampling typically includes multiple depths within the upper 50 meters, offering critical information on vertical distribution of phytoplankton biomass that complements the satellite surface observations.

https://doi.org/10.5194/egusphere-2026-3657
Preprint. Discussion started: 27 July 2026

The in situ Chl-a dataset used in this study exhibits significant spatiotemporal clustering. The temporal sampling baseline is stable, with approximately 13–85 observation points per month, but a significant anomalous peak occurs in May 2016, reaching 474 profiles, marking an intensive cross-basin field expedition (Fig. 2a). Normalized Gaussian kernel density maps show that data density is highly concentrated in the Baltic Propoer and the Gulf of Finland (Fig. 2b). The areas with the highest relative density (0.85–1.0) are concentrated at internationally recognized long-term monitoring stations, such as BY15 in the Eastern Gotland Basin, which are regularly visited for routine environmental reporting. Outside these highly surveyed corridors and long-term monitoring stations, large areas of the basin exhibit sparse spatial data gaps, indicating the typical spatial heterogeneity of sampling inherent in hybrid autonomous and shipborne marine monitoring programs.

2.2.2 Sea Surface Temperature

The SST data utilized in this study were obtained from the EUMETSAT Ocean and Sea Ice Satellite Application Facility (OSI SAF) high-latitude Level-3 Sea and Sea Ice Surface Temperature products OSI-203-a (Metop-B/AVHRR) and OSI-203-b (S-NPP/VIIRS). These products cover all ocean and ice regions poleward of 50°N and provide twice-daily gridded SST and sea ice surface temperature fields at a spatial resolution of 5 km. The dataset spans from 2012 onwards and combine clear-sky retrievals from multiple overpasses into regular daily composites, thereby effectively capturing seasonal and interannual SST variability across the Baltic Sea and adjacent high-latitude seas (Donlon et al., 2012; Merchant et al., 2019).

3. Methodology

3.1 Local Singular Evolutive Interpolated Kalman filter

We employ the Local Singular Evolutive Interpolated Kalman filter (LSEIK; Pham et al., 1998) to assimilate observations into the coupled ocean–biogeochemical model. LSEIK is an ensemble-based scheme that updates the model state by optimally combining the forecast with observations according to their respective error statistics. The analysis state vector is obtained from the forecast state through a Kalman filter update, in which the innovation (difference between observations and model equivalents) is weighted by the Kalman gain matrix. The gain is computed from the forecast error covariance and the observation error covariance, following standard ensemble Kalman filter formulations. An inflation factor of 0.3 is applied to the forecast error covariance to mitigate ensemble underdispersion. This value follows previous applications of LSEIK in ocean DA (e.g., Liu and Fu, 2018) and is adopted here as a pragmatic choice to ensure stable filter performance. The LSEIK filter is implemented in an offline configuration, where ensemble statistics are derived from a long-term free-running model simulation rather than from a dynamically evolving ensemble. This approach provides a computationally efficient estimate of background error covariances while retaining the dominant variability of the system.

https://doi.org/10.5194/egusphere-2026-3657
Preprint. Discussion started: 27 July 2026

In this study, a weakly coupled DA framework is adopted. Although physical and biogeochemical variables are included in a common state vector, they are updated independently during the analysis step, and no explicit cross-variable error covariances are imposed. As a result, interactions between biological and physical variables arise only through the nonlinear model dynamics during the forecast step, as cross-variable error covariances are not explicitly represented. Therefore, any impact of Chl-a corrections on temperature or stratification should be interpreted as an indirect effect mediated by changes in radiative transfer and subsequent physical adjustments within the model.

3.2 Localization Strategy

To reduce spurious long-range correlations in ensemble-based error covariances, spatial localization is applied to the Kalman gain. Distance-based weighting functions are used to restrict the influence of observations to a local neighborhood around each model grid point. Horizontally, we apply a Gaussian tapering function with a cutoff radius of 150 km for physical variables and 100 km for biogeochemical variables. Vertically, a uniform localization radius of 30 m is used for all variables. The observations within the localization radius are weighted based on their Euclidean distance between the observation location and the target grid points using a quasi-Gaussian function (Liu et al., 2013; Liu et al, 2021). Although this approach does not explicitly account for complex bathymetry, it provides a computationally efficient and previously validated solution for the Baltic Sea.

The choice of a uniform vertical localization radius of 30 m represents a compromise between capturing upper-ocean variability and limiting spurious vertical correlations. This value is broadly consistent with typical mixed layer depths during productive seasons in the Baltic Sea. However, the use of a constant vertical scale does not account for seasonal or regional variability in stratification, and sensitivity to this parameter remains a source of uncertainty.

3.3 Ensemble Generation and Assimilation Cycle

The LSEIK filter is implemented in an offline configuration, in which ensemble perturbations are constructed from a long-term free-running model simulation rather than being dynamically evolved. The background error statistics are estimated from a multi-decadal hindcast covering the period 1990–2016, with model snapshots stored at three-day intervals. For each analysis date, ensemble members are selected using a time-window sampling approach to represent seasonally consistent variability. Specifically, a 6-year temporal window centered on the target date is considered, and for each year within this window, model snapshots within ±45 days of the analysis date are extracted. This window length was selected to ensure sufficient sampling of interannual variability while maintaining seasonal consistency. This results in a total ensemble size of 120 members (6 years × 20 samples per year), providing a balance between sampling robustness and computational efficiency. The use of an offline ensemble derived from a long-term hindcast provides a computationally efficient approximation of background error covariances and captures dominant seasonal and interannual variability. However, this approach assumes statistical stationarity and may not fully represent transient or extreme events.

https://doi.org/10.5194/egusphere-2026-3657
Preprint. Discussion started: 27 July 2026

To isolate the dominant variability relevant for DA, the ensemble pool is first filtered using a Gaussian band-pass filter to suppress both high-frequency noise and low-frequency trends. A multivariate empirical orthogonal function (EOF) decomposition is then applied, and the leading modes are retained to define a reduced-order representation of the forecast error covariance. Ensemble perturbations are subsequently reconstructed using a second-order exact sampling method (Liu and Fu, 2018), yielding a low-rank but dynamically consistent estimate of background uncertainty.

DA is performed within a 3-day window centered on the analysis time, incorporating observations from one day before to one day after. This window represents a functional compromise between the rapid evolution of the spring bloom and the thermodynamic response time of the upper mixed layer (Stramska and Jakacki, 2024). The window is sufficiently short to capture the rapid onset and peak of phytoplankton blooms (e.g., the spring diatom bloom or summer cyanobacteria filaments; Klais et al, 2021), thereby preventing the model from significantly drifting away from the observed biomass dynamics. At the same time, this window provides sufficient integration time for the model's radiative transfer scheme to respond to the updated chlorophyll fields. Specifically, chlorophyll concentration updates modify the light attenuation coefficient, which alters the vertical distribution of shortwave radiation and consequrently contribute to changes in the temperature tendency (Ciavatta et al., 2018, Skákala et al., 2021). A multi-day forecast is therefore required for these localized heating rate anomalies to translate into a measurable change in thermal structure (Gentemann, et al. 2009; Kang e al, 2024).

This weakly coupled assimilation framework circumvents the known issues in strongly coupled system, where poorly constrained or non-stationary cross-variable covariances can introduce spurious correlations or initialization shock. In our setup, the 3-day forecast acts as a natural physical-biogeochemical filter, ensuring that any indirect thermodynamic updates remain dynamically consistent with the model's internal physics.

To reduce computational cost, ensemble perturbations are updated at different temporal frequencies for different variable groups: every 6 days for physical variables and every 30 days for biogeochemical variables. This approach reflects the faster temporal variability of physical processes compared to biogeochemical dynamics, while maintaining computational efficiency.

3.4 Observation Quality Control and Error Specification

All observations undergo a series of quality control procedures prior to assimilation. Observations located over land, as defined by the model land–sea mask, are excluded, along with duplicate records. Satellite observations within 5 km of the coastline are removed to reduce contamination from land adjacency effects. When multiple observations are available within the same model grid cell and depth level, they are averaged to provide a representative value.

https://doi.org/10.5194/egusphere-2026-3657
Preprint. Discussion started: 27 July 2026

The observation error covariance matrix is assumed to be diagonal, implying uncorrelated observation errors. Observation error standard deviations are specified according to variable type and data source. For SST, a constant error standard deviation of 0.3 °C is adopted, consistent with previous regional DA studies (Liu and Fu, 2018). Chl-a observations are assimilated in logarithmic space to account for their approximately log-normal distribution and to ensure non-negativity. For in situ Chl-a profiles, a constant error standard deviation is assumed in log-space, defined as:

$$\sigma_{in\_situ} = \log(1 + 0.1) \quad (1),$$

corresponding to an approximate relative uncertainty of 10%, reflecting a stable measurement uncertainty. For satellite-derived Chl-a, the observation error is formulated as a function of the observed concentration to account for increased uncertainty at low concentrations and in optically complex waters. The standard deviation in log-space is defined as follows:

$$R = \log\left(1 + \max(\varepsilon_{rel}, \frac{0.1}{C_{obs}})\right) \quad (2),$$

where C_{obs} denotes the observed Chl-a concentration, and ε_{rel} is a sub-basin–specific relative error coefficient. The sub-basin–specific relative error coefficient (ε_{rel}) was estimated from statistical comparisons between collocated satellite and in situ Chl-a observations. For each sub-basin, relative differences were computed and aggregated to determine representative uncertainty levels, reflecting both retrieval errors and regional optical complexity. The resulting values are intended to provide a first-order characterization of spatially varying observational uncertainty.

This formulation allows the observation error to scale with concentration while avoiding unrealistically small uncertainties at low values. It also accounts for the increased uncertainty of satellite retrievals in optically complex waters such as the Baltic Sea, where high CDOM and suspended sediments can significantly affect optical signals.

It should be noted that the specification of observation errors remains a key source of uncertainty in the assimilation system, particularly for satellite-derived Chl-a. Our pragmatic parameterization attempted to balance observational constraints and model stability, but its impact on assimilation performance should be considered when interpreting the results.

3.5 Experimental Design

Based on the model configuration and DA framework described above, three numerical experiments were conducted using NEMO–SCOBI to assess the impact of DA on ecosystem dynamics. All experiments were integrated over the period from October 2015 to November 2018. Initial and restart fields for all experiments were taken from the ocean reanalysis described by von Schuckmann et al. (2019). The experiments differ only in the assimilated observations.

The reference experiment (REF) was a free-running simulation without DA and serves as a baseline representation of coupled physical–biogeochemical variability. In the CHL_SAT experiment, only satellite Chl-a observations were assimilated to constrain biogeochemical state variables and evaluate the impact of surface biogeochemical assimilation on

https://doi.org/10.5194/egusphere-2026-3657
Preprint. Discussion started: 27 July 2026

ecosystem dynamics. In the CHL_3D run, Chl-a observations from both satellite and in situ sources were assimilated to isolate the impacts of increased subsurface observational constraints on biogeochemical dynamics. In the CHL_SST experiment, both satellite and in situ Chl-a observations were assimilated alongside SST observations within the weakly coupled LSEIK framework to assess the combined influence of biogeochemical and physical constraints on coupled physical–ecosystem processes.

3.6 Assessment metrics

The experiments are evaluated against observational products using standard statistical measures, including mean bias (Bias), root mean square error (RMSE), and Taylor skill score (TSS). In addition, spatial variations between the simulations are further examined by calculating the direct differences (Δ), defined as the respective DA runs minus the REF run (e.g., CHL_SAT - REF).

These metrics are defined as follows:

$$\text{Bias} = \frac{1}{N}\sum_{i=1}^{N}\left(S_{\text{obs}}^{i} - S_{\text{sim}}^{i}\right) \quad (3),$$

$$\text{RMSE} = \sqrt{\frac{1}{N}\sum_{i=1}^{N}(S_{\text{obs}}^{i} - S_{\text{sim}}^{i})^{2}} \quad (4),$$

where S_{sim} and S_{obs} denote simulated and observed fields, respectively, and N is the total number of data points.

$$\text{TSS} = \frac{4(1+R)^{2}}{(\sigma_{\text{sim}}/\sigma_{\text{obs}}+\sigma_{\text{obs}}/\sigma_{\text{sim}})^{2}(1+R_{0})^{2}} \quad (5),$$

where R is the Pearson correlation coefficient between the simulated and the observed data, R_0 is the maximum achievable correlation coefficient (assumed to be 1 here), and σ_{sim} and σ_{obs} represent the standard deviation of simulated and observed fields, respectively.

4 Results

4.1 Sea Surface Temperature

The reference simulation (REF) reproduces the broad SST climatology of the Baltic Sea, with TSSs ranging from 0.94 to 0.99 across most sub-basins and a basin-wide temporal correlation of about 0.98 (Fig. 3a). Skill is lower in the Bothnian Bay and along the northeastern coastal margins of the Baltic Proper, where complex ice-edge dynamics and freshwater inputs are not well represented in the free run. Assimilating Chl-a alone (CHL_SAT, CHL_3D) produces only marginal changes in SST relative to REF, with spatially heterogeneous response and a negligible basin-mean TSS decrease of approximately -1.4×10^{-5} (Fig. 3b-c). This indicates that, in this weakly coupled framework, biological updates do not propagate directly into surface temperature fields. In contrast, the CHL_SST experiment achieves the highest SST skill (Fig. 3d). TSS is improved in nearly all sub-basins, except for narrow coastal zones where values remain slightly below those of REF, and basin-wide skill increases by approximately 7%, with the strongest gains in the northern Baltic Sea. These findings indicate

https://doi.org/10.5194/egusphere-2026-3657
Preprint. Discussion started: 27 July 2026

that direct SST constraints eliminates the regional cold biases present in REF and provides a physical consistent baseline for interpreting the biogeochemical state.

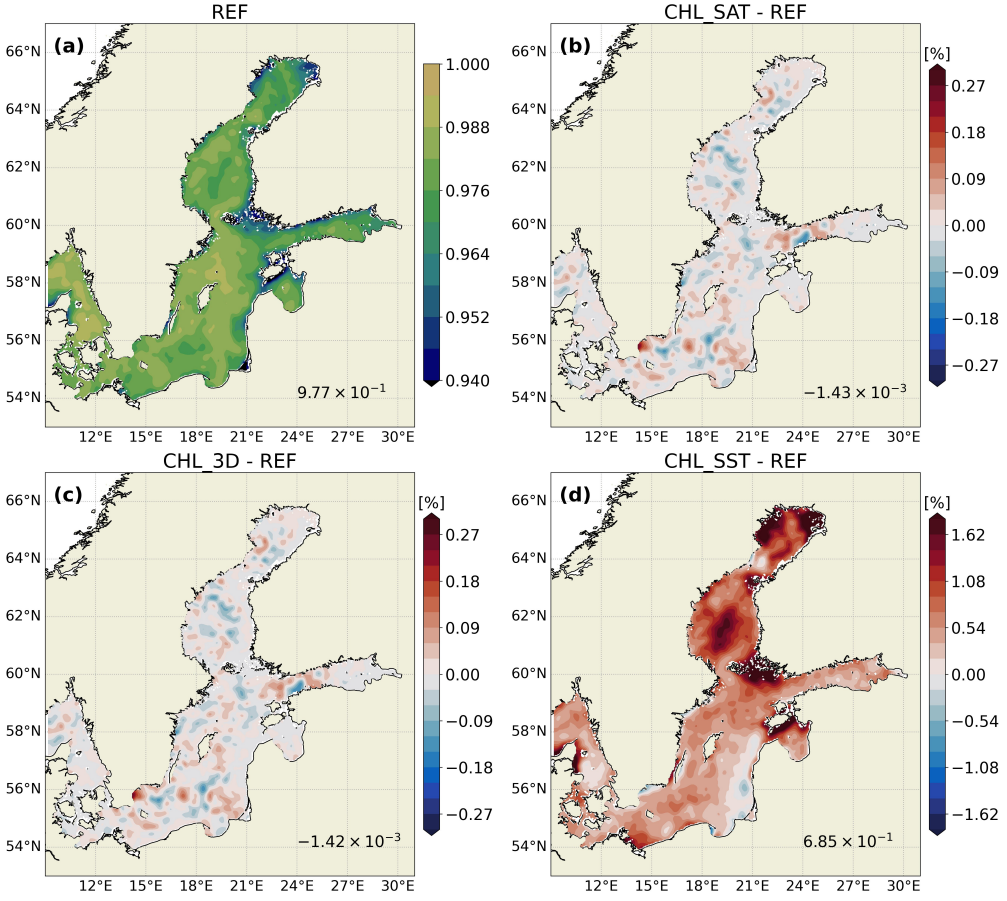

Figure 3. Spatial distribution and comparison of the Taylor Skill Score (TSS) for simulated sea surface temperature across different assimilation experiments. (a) Absolute TSS for the reference run (REF). (b–d) Spatial discrepancies in TSS (ΔTSS) between the data assimilation runs and the reference run, calculated as: (b) CHL_SAT - REF, (c) CHL_3D - REF, and (d) CHL_SST - REF. The domain-averaged value for each experiment is indicated in the upper-left corner of each panel. The colorbars in (b–d) denote the relative differences expressed in percentage (%).

These results demonstrate that incorporating physical constraints into CHL_SST allows for the developement of a more accurate thermal environment, which is a prerequisite for correctly representing the stratification-dependent processes such as bloom initiation, SCM formation, and oxygen dynamics, which are examined in the following sections. The subsequent thermal response to biological corrections is therefore interpreted as a secondary, nonlinear adjustment within the model rather than a basin-scale physical reorganization.

https://doi.org/10.5194/egusphere-2026-3657
Preprint. Discussion started: 27 July 2026

4.2 Surface Chlorophyll-a

4.2.1 Basin-Scale Assessment and Error Statistics

The REF simulation exhibits a systematically underestimation of surface Chl-a concentration across the entire basin, yielding a basin-wide RMSE of 2.30 mg m^{-3} relative to the multi-sensor satellite product. The spatial distribution of model errors shows a clear south–north gradient (Fig. 4). Performance is relatively better in the Arkona and Bornholm basins, where localized RMSE values are around 1.44 mg m^{-3}, but errors rise significantly toward the northeastern Baltic, reaching 4.02 mg m^{-3} in the Gulf of Finland and 4.62 mg m^{-3} in the Gulf of Riga. These regions characterized by intricate complex circulation, strong riverine discharge, and high CDOM concentrations.

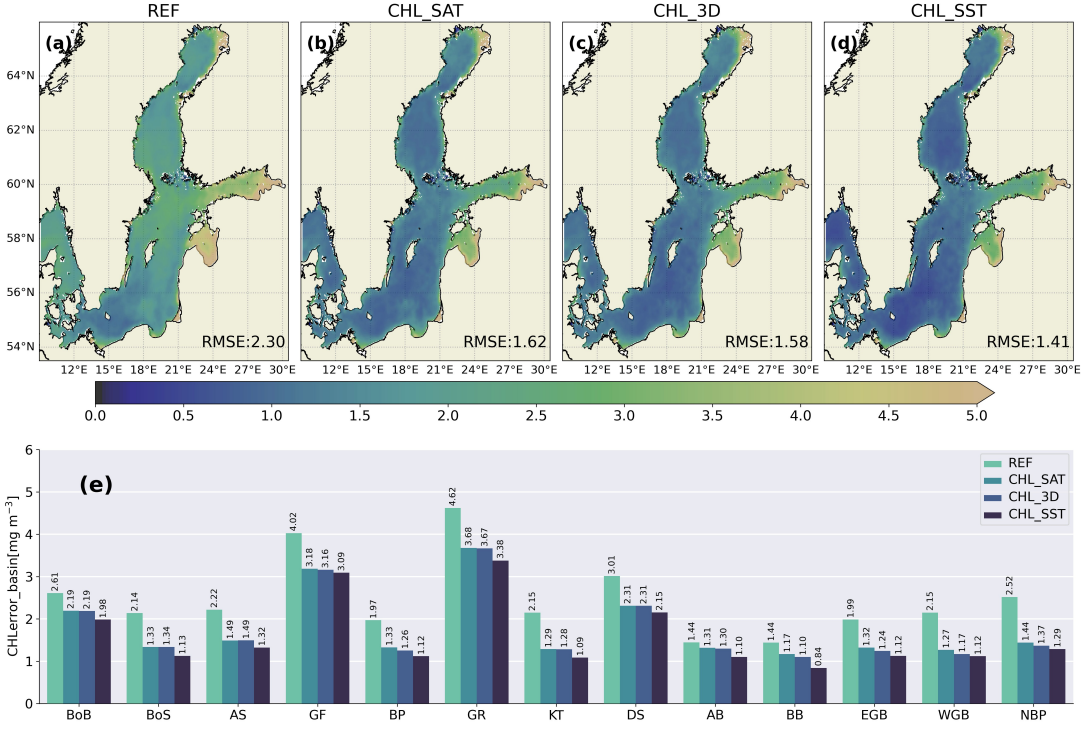

Figure 4. Spatial and regional assessment of modeled surface chlorophyll-a errors. (a–d) Spatial distribution of root-mean-square error (RMSE, mg m^{-3}) calculated against the multi-sensor satellite product for the reference run and the respective data assimilation experiments. (e) Regional comparison of the domain-averaged RMSE (mg m^{-3}) across the major sub-basins of the Baltic Sea.

All three DA configurations substantially reduce the basin-mean RMSE, although with varying efficienicy. CHL_SAT decreases the Baltic-mean RMSE to 1.62 mg m^{-3}, correponding a 30% reduction relative to REF, while CHL_3D performs slightly better with a RMSE of 1.58 mg m^{-3} (a 31% reduction). The largest local improvement in CHL_3D occurs in the

https://doi.org/10.5194/egusphere-2026-3657
Preprint. Discussion started: 27 July 2026

northern Baltic Proper and West Gotland Basin, where localized RMSE decreases by 46% and 45%, respectively. The CHL_SST experiment provides the most robust constraint, further reduces basin-mean RMSE to 1.41 mg m^{-3} (a 39% reduction relative to REF). These quantitative reductions show that the northern sub-basins, Arkona Basin, and Bornholm Basin benefit most from the combined physical and biogeochemical constraint. The comparison also suggests that the physical and biogeochemical constraints are complementary rather than redundant. Regions that benefited from Chl-a assimilation alone show further improvement when the SST constraint is added. This is particularly evident in northern sub-basins, where stratification dictates bloom phenology, and within the Arkona and Bornholm basins, where complex hydrodynamic features amplify the impact of thermal assimilation. In these regions, the SST assimilation appears to correct the upper-ocean thermal environment that regulates phytoplankton development, while Chl-a assimilation directly constrains biomass.

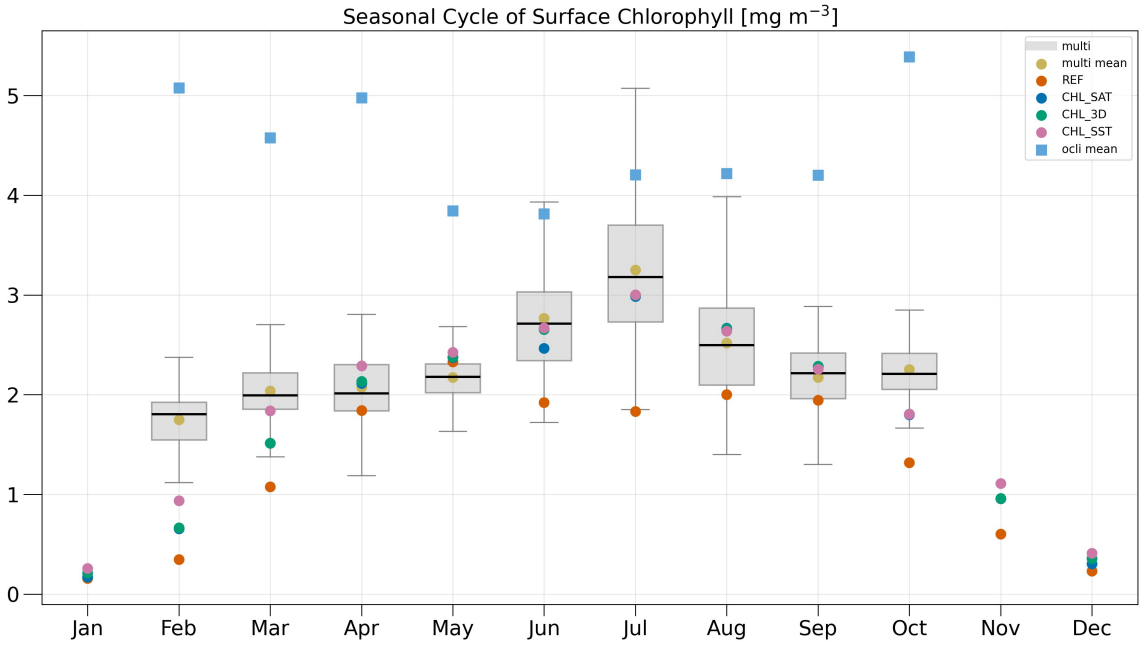

Figure 5. Seasonal variability of surface Chlorophyll-a (mg m^{-3}) from the four numerical experiments and two observational products (multi-sensor and Sentinel-3) in the Baltic Sea.

A comparative analysis of the two satellite Chl-a products reveals distinct differences in seasonal amplitudes. The multi-sensor product yields a summer maximum of approxmiately 3.4 mg m^{-3}, whereas Sentinel-3 reports consistently higher concentrations, characterized by an enhanced late-winter to early-spring signal (Fig. 5). None of the DA experiments are capable of replicating this early-season peak in Sentinel-3 product. This persistent mismatch originates from a hard-coded structural thresholding within the biogeochemical formulation rather than a failure of the assimilation scheme itself (Eilola et al, 2009; Ruvalcaba Baroni et al., 2024). Specifically, overly restrictive thresholds for minimum light availability and

https://doi.org/10.5194/egusphere-2026-3657
Preprint. Discussion started: 27 July 2026

background phytoplankton biomass artificially suppress primary production under cold, low-light, early-season conditions. Therefore, this limits the model's intrinsic ability to initiate the late-winter to early-spring bloom, regardless of the strength or configuration of the observational constraints applied.

4.2.2 Seasonal spatial distribution

The impact of assimilation on the spatial distribution of simulated surface Chl-a shows a clear seasonal divergence, indicating the evolving interplay between thermodynamic forcing and biological growth regimes that govern chlorophyll dynamics in the Baltic Sea (Fig. 6). In winter, robust convective mixing supplies abundant ambient nutrients, but severe light limitation and low temperature suppress phytoplankton growth, resulting in minimal biomass. During this period, the model shows its maximum annual basin-wide bias (1.68 mg m^{-3}). Although satellite observation quality deteriorates due to sea-ice cover and cloud contamination, DA runs reduce errors by 8–18% relative to the free run. Notably, assimilating SST data yields an error reduction approximately 1.8 times greater than that achieved through the biological constraints alone, implying that correcting the thermodynamic state is more effective under extreme light-limited conditions. In spring, the dynamics of phytoplankon bloom in the Baltic Sea are primarily governed by mixed-layer shoaling and light availability. Under these conditions, CHL_SST reduces the Chl-a bias by 64%, substantially outperforming the 38% reduction achieved by assimilating biological observations alone (CHL_SAT). This disproportionate improvement indicates that maintaining an accurate thermal and stratification state is a critical prerequisite for capturing bloom onset and spatial distribution. In summer, nutrient limitation (i.e., nitrogen and phosphorus) becomes the dominant control governing phytoplankton dynamics, especially in the central and southern Baltic basins. Direct biological assimilation in CHL_SAT reduces the Chl-a bias by 64%, particularly in the Baltic Proper, where the bias decreases from 0.61 to 0.12 mg m^{-3}. Because the upper-ocean physical structure is relatively stable at this stage, additional SST constraints provide only marginal benefits, implying that improvements are driven mainly by the direct correction of biogeochemical states. In autumn, enhanced vertical mixing triggers a secondary bloom by entraining nutrients from the deeper layers. The REF run shows considerable biases in productive coastal regions, with a basin-wide mean bias of 1.36 mg m^{-3}. All DA configurations reduce these biases by 29–32%, though residual errors persist in highly productive nearshore areas.

https://doi.org/10.5194/egusphere-2026-3657
Preprint. Discussion started: 27 July 2026

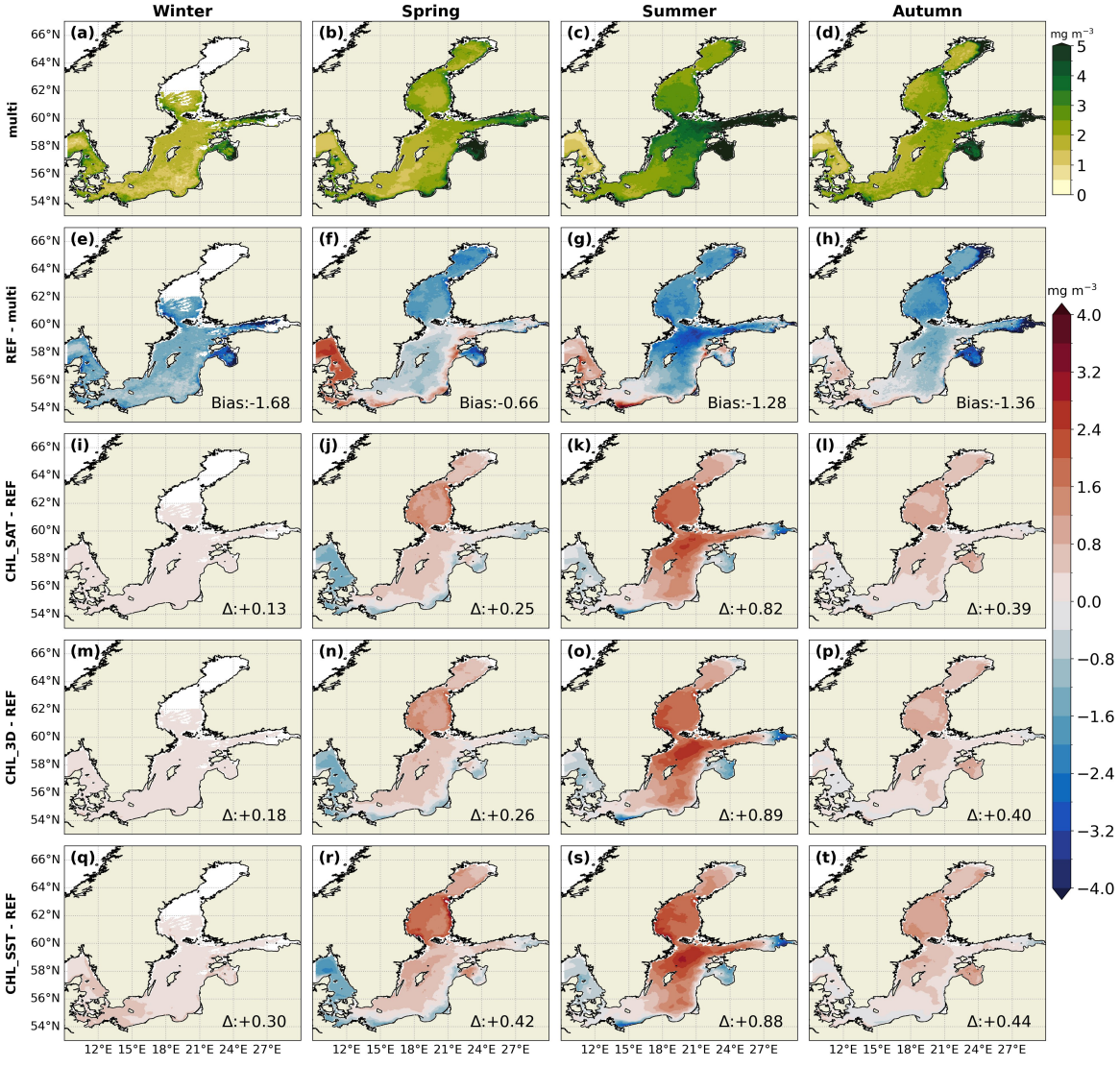

Figure 6. Seasonal spatial distribution of surface chlorophyll-a concentrations and discrepancies across different simulation experiments. (a–d) Multi-sensor satellite observational product used as the reference baseline for Winter, Spring, Summer, and Autumn, respectively. (e–h) Spatial mean bias (Bias, mg m^{-3}) of the reference run (REF) relative to the satellite product (multi - REF). (i–t) Spatial differences (Δ, mg m^{-3}) in surface chlorophyll-a between the respective data assimilation (DA) runs and the REF run, calculated as: (i–l) CHL_SAT - REF, (m–p) CHL_3D - REF, and (q–t) CHL_SST - REF. The domain-averaged value for each specific case is indicated in the upper-left corner of each panel.

https://doi.org/10.5194/egusphere-2026-3657
Preprint. Discussion started: 27 July 2026

Overall, these seasonal patterns indicate a systematic shift in dominance constraint on model skill for phytoplankton dynamics in the Baltic Sea. Physical constraint is most important in winter and spring, while biological constraint becomes more important in summer and autumn.

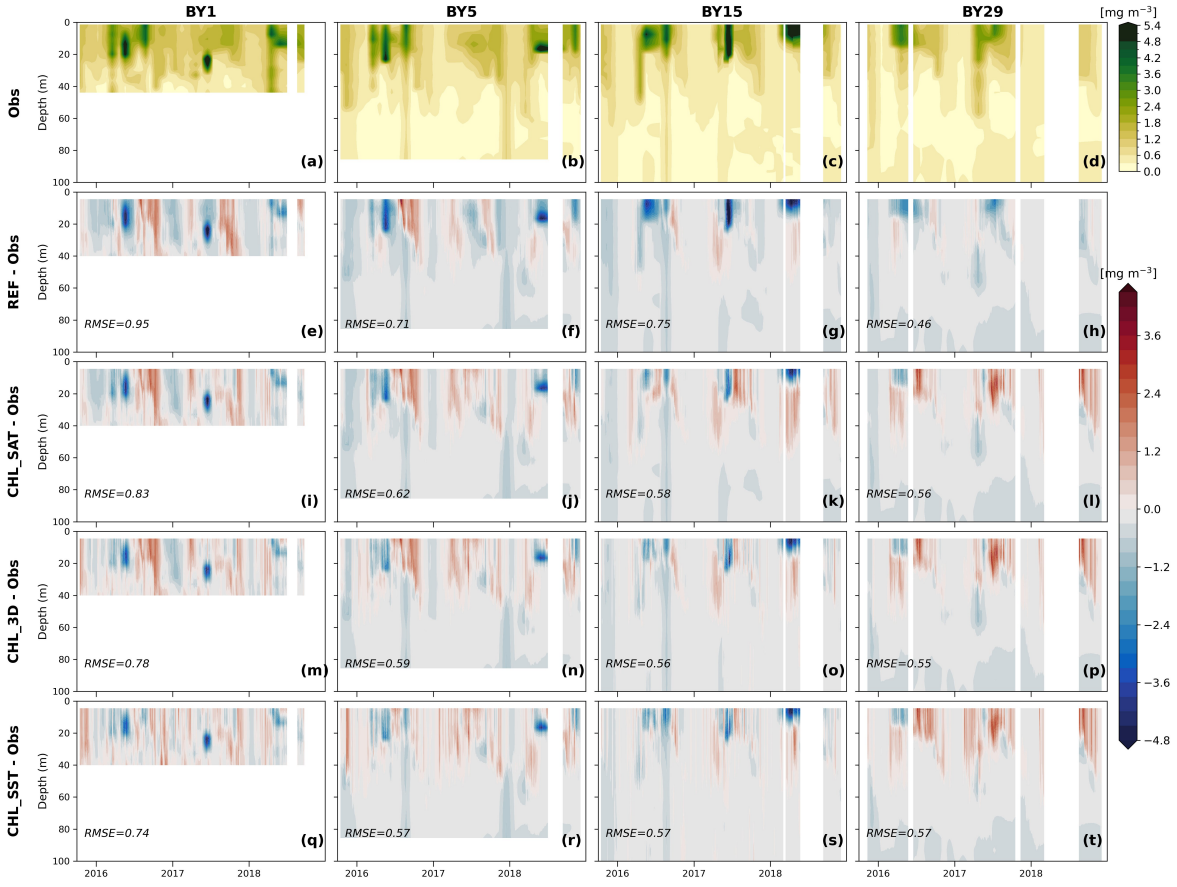

Figure 7. Time–depth distributions of chlorophyll-a across major Baltic sub-basins. Comparison between in situ observations (first row) and simulation experiments: REF (second row), CHL_SAT (third row), CHL_3D (fourth row), and CHL_SST (fifth row). Stations represent a south–north gradient: BY1 (Arkona Basin), BY5 (Bornholm Deep), BY15 (Eastern Gotland Basin), and BY29 (Northern Baltic Proper). Note the enhanced representation of the Subsurface Chlorophyll Maximum (SCM) in the CHL_3D and CHL_SST experiments following the inclusion of vertical profile data.

https://doi.org/10.5194/egusphere-2026-3657
Preprint. Discussion started: 27 July 2026

4.3 Vertical Chlorophyll-a Structure

4.3.1 Satellite-only assimilation and its vertical limitations

Assimilating satellite-derived Chl-a (CHL_SAT) markedly improves the simulation of surface bloom dynamics, better constraining bloom timing and magnitude within the mixed layer (Figs. 7 and 8). However, the impact of surface observations on subsurface layers is limited by vertical localization. Rather than propagating improvements downward, the surface-bounded constraint occasionally generates spurious vertical gradients and fails to correct the subsurface chlorophyll structure. In particular, the CHL_SAT remains incapable of accurately reproducing the SCM during stratified periods, which fluctuates between 15 and 30 m based on in situ observations. In contrast, the SCM inferred from the CHL_SAT run persists near the surface, similar to the REF run. This vertical decoupling is a fundamental consequence of the observation geometry. Satellite sensors sample only the uppermost optical depth ($\sim 1/K_d$), whereas the SCM forms near the base of the seasonal pycnocline at depths of about 20–40 m in the central Baltic.

https://doi.org/10.5194/egusphere-2026-3657
Preprint. Discussion started: 27 July 2026

Figure 8. Simulated vertical profiles of chlorophyll-a (Chl-a, mg m^{-3}) temporal evolution revealing the dynamics of Subsurface Chlorophyll Maxima (SCM) from 2016 to 2019 at stations BY1, BY5, BY15, and BY29. Columns correspond to the different monitoring sites, whereas rows display the four numerical experiments. The results demonstrate the capability of the three-dimensional assimilation schemes (CHL_3D and CHL_SST) in reconstructing the seasonal deepening and structural stratification of the phytoplankton biomass within the euphotic zone compared to the surface-only constraint (CHL_SAT).

The basin-wide profile validation (Table 1) quantifies a localized degradation in the subsurface layers, where the basin-mean bias in the CHL_SAT run worsens relative to that in the REF run (increasing from 0.14 to 0.62 mg m^{-3} at 5–10 m and from 0.49 to 0.68 mg m^{-3} at 10–20 m). However, the seasonal mean profiles at representative offshore stations show that the satellite assimilation better resolves the observed mixed layer depth relative to the REF run(Fig. 9). This discrepancy implies that the subsurface degradation is spatially localized and primarily driven by productive coastal zones and river plumes unresolved by the offshore stations.

https://doi.org/10.5194/egusphere-2026-3657
Preprint. Discussion started: 27 July 2026

Table 1. Basin-wide statistical validation of simulated Chlorophyll-a (mg m^{-3}). Statistical performance metrics – Root Mean Square Error (RMSE) and Mean Bias (Bias) – calculated against all available in situ observations (0–200 m) for the entire Baltic Sea.

Depth Range	Metrics(mg m^{-3})	REF	CHL_SAT	CHL_3D	CHL_SST
Surface (0–5m)	RMSE	5.51	5.36	5.23	5.16
	Bias	1.18	1.14	1.37	1.30
Mid (5–10m)	RMSE	3.19	2.78	2.68	2.62
	Bias	0.14	0.62	0.39	0.33
Mid (10–20m)	RMSE	1.85	1.72	1.43	1.40
	Bias	0.49	0.68	0.16	0.16
Mid (20–30m)	RMSE	1.85	1.76	1.49	1.51
	Bias	0.96	0.75	0.34	0.29
Mid (30–40m)	RMSE	0.88	0.83	0.75	0.79
	Bias	0.37	0.17	0.13	0.05
Deep (>40m)	RMSE	0.23	0.20	0.14	0.15
	Bias	0.18	0.10	0.05	0.03

4.3.2 Profile assimilation and SCM reconstruction

Incorporation of in situ Chl-a profiles (CHL_3D and CHL_SST) significantly enhances the representation of the vertical biomass distribution, reducing the systemic subsurface chlorophyll overprediction occurred in unconstrained simulation (Table 1). The largest improvement occurs in intermediate layers (10–20 m), where both profile-based assimilation configurations reduce the basin-mean bias by 67%, from 0.49 mg m^{-3} in REF to 0.16 mg m^{-3}. Additionally, a 34% reduction in RMSE is achieved in waters below 40 m. The seasonal evolution of the SCM depth (Fig. 8) shows that both CHL_3D and CHL_SST effectively guide the biomass peak to descend into the pycnocline (approximately 15–30 m) during summer stratification, with reducing localized profile RMSE reduction of up to 25% at station BY15 (Fig. 7). This behavior indicates that in situ profiles directly constrain the depth-integrated phytoplankton structure that governs light attenuation, nutrient drawdown, and oxygen consumption. This adaptive capability is further evident in their precise responsiveness to transient hydrodynamic forcing. During episodic mixing, such as early 2018 at station BY29, these constraints promptly induce sharp downward shift in SCM following a mixing event (Fig. 8).

https://doi.org/10.5194/egusphere-2026-3657
Preprint. Discussion started: 27 July 2026

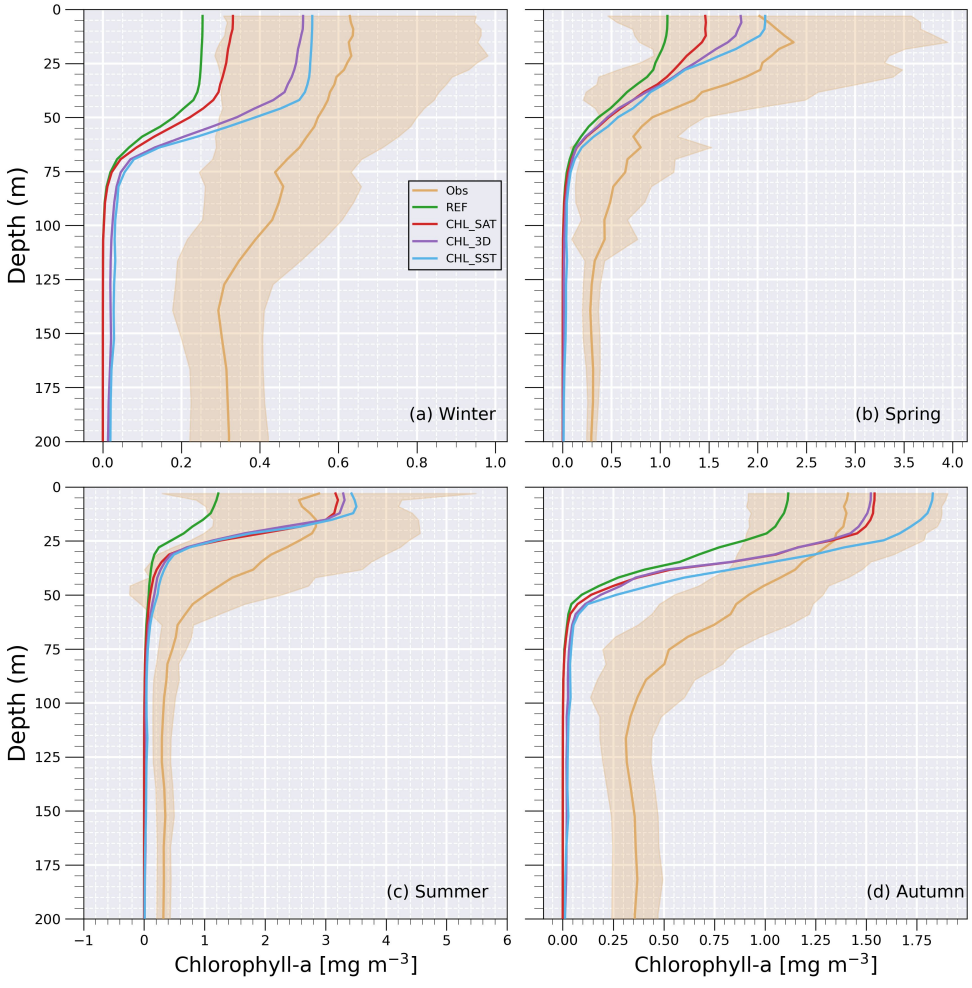

Figure 9. Seasonal evolution of Chlorophyll-a at representative monitoring stations. The mean vertical profiles of observations and simulations are show for stations BY1, BY5, BY15, and BY29. The data assimilation experiments successfully correct the timing and magnitude of the spring bloom. Each panel represents one season (Winter, Spring, Summer, Autumn), with station variability captured in the shaded regions for observations and mean profiles plotted for simulations.

Seasonal mean profiles (Fig. 9) show the greatest RMSE reductions occur in spring and summer, whereas autumn mixing reveals a clear difference between the two profile-constrained configurations. As autumnal convection deepens the mixed layer, both the CHL_3D and CHL_SST runs sustain their vertical responsiveness, successfully guide the simulated SCM downward into intermediate depths (approximately 15–30 m). However, the REF and CHL_SAT runs fail to adapt to this vertical feature. Furthermore, a distinct vertical partitioning emerges between the two profile-constrained configurations. The CHL_3D run primarily optimizes the water column within the upper 30 m, whereas the CHL_SST run provides a more

https://doi.org/10.5194/egusphere-2026-3657
Preprint. Discussion started: 27 July 2026

accurate structural representation of the deeper chlorophyll features in the 30–55 m depth range. This divergence suggests SST assimilation indirectly regulates the subsurface ecosystem during the autumn transition by correcting the underlying thermodynamics and accurately modulating the seasonal pycnocline.

4.4 Bio-optical Feedbacks and Thermal Response

The direct SST constraints in Section 4.1 provide the large-scale physical baseline for the analysis. Here, we examine the localized thermal response that arises from biological correction alone. Correcting the biological state through Chl-a assimilation produces physically consistent changes in the vertical thermal structure, even without the direct temperature updates. Figure 10 illustrates this bio-optical feedback at stations BY5 in the Bornholm Basin and BY15 in the Eastern Gotland Basin during the post-spring bloom period (May). In the REF run, the underestimated phytoplankton biomass yields a relatively transparent water column, with K_d values of about 0.20–0.22 m^{-1} in the upper 25 m. The CHL_SAT run increases K_d to around 0.23 m^{-1} at BY5 and about 0.25 m^{-1} at BY15, indicating stronger optical attenuation. These optical modifications redistribute solar heating vertically. Although overall SSTs remain nearly unchanged across the Chl-a–only assimilation experiments, the increased turbidity in CHL_SAT induces a localized, modest near-surface warming of up to 0.4 °C and a slight cooling in the intermediate layer between 25 and 75 m relative to the REF run. This vertical pattern is consistent with the expected response to enhanced biological shading. Below 75 m, temperature profiles converge across Chl-a–only assimilation experiments. This convergence demonstrates that the thermal feedback is confined to the depth range controlled by seasonal stratification and the penetration depth of shortwave radiation.

https://doi.org/10.5194/egusphere-2026-3657
Preprint. Discussion started: 27 July 2026

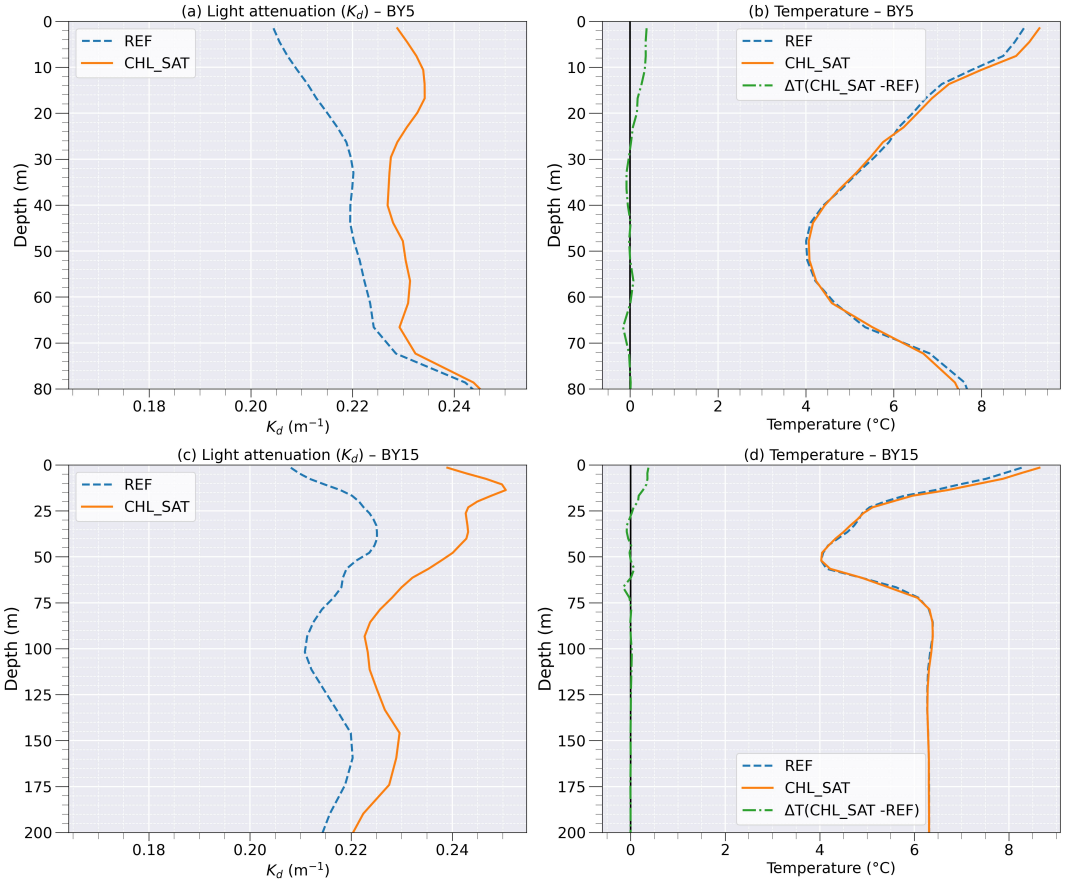

Figure 10. Vertical profiles of the light attenuation coefficient (K_d, m^{-1}) and temperature (°C) at monitoring stations (a–b) BY5 (Bornholm Basin) and (c–d) BY15 (Eastern Gotland Basin) in May. The CHL_SAT experiment shows higher K_d and an approximately 0.4 °C deep-water warming compared to the REF run. This divergence highlights a physical–biogeochemical feedback where corrected biological turbidity modifies the vertical distribution of solar radiation absorption, leading to localized adjustments in the mixed layer depth and the sequestration of heat in subsurface layers.

The resulting thermal changes are small and spatially heterogeneous, and they do not lead to a basin-wide improvement in SST statistics (TSS change < 0.01%). This near-neutral response suggests that the bio-optical feedback primarily redistributes heat vertically rather than driving large-scale surface temperature anomalies. In salinity-stratified marginal seas like the Baltic Sea, buoyancy and horizontal gradients are primarily influenced by wind mixing and riverine inputs, which dominate the weaker thermodynamic signatures of biological light absorption.

https://doi.org/10.5194/egusphere-2026-3657
Preprint. Discussion started: 27 July 2026

4.5 Deep dissolved oxygen

The vertical distribution of dissolved oxygen at the four monitoring stations reveals a clear two-layer structure, which is distinctly insensitive to the choice of DA configuration (Fig. 11). Within the well-ventilated upper mixing and oxic waters (0–40 m), all simulations show a narrow variability and systematically slightly overestimate dissolved oxygen compared to shipboard observations by 0.5–1.5 ml L^{-1}. The biological DA configurations achieve a visible reduction in this positive bias. This improvement proves that an enhanced representation of biomass and subsurface thermal signatures leads to more accurate dissolved oxygen distributions in oxic waters. Notably, the inter-comparison of these experiments reveals introducing surface thermal constraints yields further error reduction in these oxic intermediate layers, highlighting the synergistic benefit of joint physical–biogeochemical corrections on upper-ocean redox state variables. A profound departure from observations occurs beneath the pycnocline. In the deep basins, below 75m, all simulations fail to reproduce the observed sharp oxycline, showing a persistent positive oxygen bias of 1.0–2.5 ml L^{-1} before transitioning into anoxic conditions (Fig. 11c–d), where the negative values represent the equivalent hydrogen sulfide (H_2S) debt. The assimilation runs show slightly larger discrepancies from observations than the REF run in these hypoxic layers, whereas the spread among configurations remains very small. This behavior indicates that improving surface biological forcing and upper-ocean bio-optical feedbacks does not improve the representation of the deep oxycline. This finding mechanistically implicates physical transport (particularly the episodic saltwater inflows that ventilate the deep basins) and sediment remineralization as the primary controls on the vertical oxygen gradient, processes not constrained by current DA framework.

https://doi.org/10.5194/egusphere-2026-3657
Preprint. Discussion started: 27 July 2026

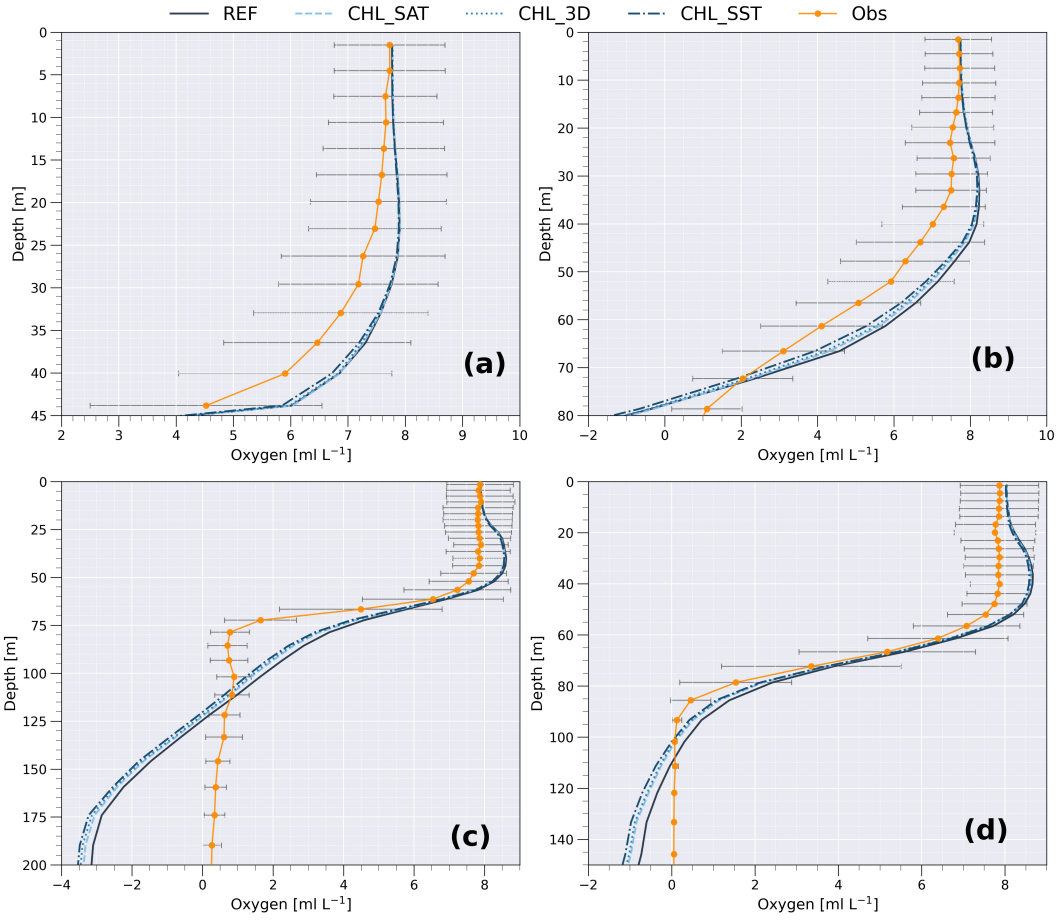

Figure 11. Comparison of simulated vertical profiles of the dissolved oxygen (ml L^{-1}) against in situ observations at monitoring station (a) BY1 (Arkona Basin), (b) BY5 (Bornholm Basin), (c) BY15 (east Gotland Basin), and (d) BY29 (north Baltic proper). Horizontal error bars on the in situ observation represent observational uncertainty. Note the high model-observation agreement in the upper 20 m (oxic zone) and the increasing model bias and observational uncertainty within the oxycline (50–100 m), particularly in the deeper basins (c and d).

The persistently wide observational uncertainty in the 50–100 m oxycline zone also warrants caution in the quantitative interpretation of model-data mismatch at depth. These results delineate the boundaries of what surface-focused, weakly coupled DA. This framework can effectively improve the biological and thermal state of the euphotic zone. However, the redox environment of the deeper basins is governed by internal model dynamics and requires independent physical or deep-water constraints to be improved.

https://doi.org/10.5194/egusphere-2026-3657
Preprint. Discussion started: 27 July 2026

5 Discussion

5.1 Asymmetry of Biophysical Coupling in Halocline-Dominated Marginal Seas

Our experiments demonstrate a pronounced asymmetry in biophysical coupling pathways in the Baltic Sea. Physical constraints strongly regulate ecosystem evolution through their control of stratification, mixing, and nutrient supply, whereas biological corrections exert a localized and vertically confined influence on the thermal structure. Previous Baltic Sea studies have shown that optically active constituents can alter the vertical distribution of shortwave heating but produce only a weak SST response under strong stratification and efficient wind-driven mixing (Löptien and Meier, 2011; Cahill et al., 2023). Here, we extend these findings by separating physical control on ecosystem dynamics from the thermal response to biological corrections, allowing the direction and strength of biophysical coupling to be evaluated explicitly in a single modeling framework.

In the CHL_SAT and CHL_3D experiments, enhanced phytoplankton biomass increases light attenuation, leading to a weak surface warming and a compensating subsurface cooling (25–75 m). This vertical dipole structure, consistent with previous global and regional bio-optical feedback studies (Manizza et al., 2005; Lengaigne et al., 2007; Park et al., 2014; Hernandez et al., 2017; Berthet et al., 2023; Meng et al., 2024), indicates a redistribution of heat rather than a substantial change in upper-ocean heat content. Although the biologically induced temperature anomalies remain small (< 0.4 °C), they may still modify the local density gradients near the thermocline and influence the timing of seasonal mixed-layer deepening. In a halocline-dominated marginal sea, such perturbations may advance the onset of autumn mixing, with implications for nutrient entrainment and oxygen ventilation across the oxycline. In a seasonally stratified and oxygen-sensitive system such as the Baltic Sea, ecological sensitivity may exceed thermal sensitivity, with small thermal perturbations influencing nutrient supply, oxygen ventilation, and the timing of seasonal transitions. These mechanistic insights go beyond earlier Baltic studies, which mostly focused on the physical response to optical properties rather than on the coupling between physical control and biological feedbacks (Löptien and Meier, 2011; Cahill et al., 2023). The weak thermal response contrasts with more weakly stratified systems, in which bio-optical feedbacks can more readily alter the thermal state(e.g., Löptien et al, 2009; Gnanadesikan and Anderson, 2009; Park et al., 2014). The difference likely arises from the dominant role of salinity stratification in the Baltic Sea. The permanent halocline preconditions the upper-ocean heat budget and limits the penetration of optical perturbations, thereby suppressing the translation of chlorophyll variability into basin-scale thermal anomalies. As a result, chlorophyll variability modifies the vertical heat structure without substantially altering the horizontal temperature patterns.

The CHL_SST result further clarifies this asymmetry. SST assimilation reduces regional cold bias and improves the physical environment governing phytoplankton dynamics. Chlorophyll assimilation produces only a minor thermal adjustment, while significantly correcting phytoplankton biomass. The weak thermal response indicates the dominance of the pre-existing

https://doi.org/10.5194/egusphere-2026-3657
Preprint. Discussion started: 27 July 2026

hydrographic structure in regulating the expression of bio-optical feedbacks. Accordingly, the thermal response to biological assimilation should be interpreted as a secondary, dynamically consistent adjustment within a halocline-dominated system rather than as a basin-scale reorganization of surface temperature. Biophysical coupling in the Baltic Sea is therefore not weak but strongly asymmetric, with physical forcing dominating biogeochemical variability and biological feedbacks exerting only a secondary influence on the thermal state. The pronounced asymmetry in coupling pathways provides a mechanistic basis for designing observation-sensitive assimilation strategies in halocline-dominated coastal seas.

5.2 Vertical mediation of surface biogeochemical change

The differences among assimilation runs suggest that surface biogeochemical anomalies in the Baltic Sea are not propagated linearly downward through the water column, but are mediated by the contemporaneous thermal state and stratification of the upper water column (Berthet et al., 2023). Accordingly, chlorophyll variability should be considered as a process outcome. This outcome is conditionally expressed within a vertically structured physical environment (Viljoen et al, 2024). Our multi-experiment configuration provides a direct diagnostic platform to test this coupling. By isolating the independent impacts of thermal and biological constraints, we can resolve the precise environmental thresholds where surface data ingestion successfully translates into vertical subsurface precision.

Our findings indicate that the capacity of surface chlorophyll corrections to penetrate downward depends on whether the upper ocean maintains sufficient vertical coherence. Satellite-only assimilation (CHL_SAT) can improve near-surface bloom signals, but it remains less effective at constraining the SCM during transition periods (Wang et al., 2021). While expanding this biological constraint via full vertical bioprofile assimilation (CHL_3D) extends the biological correction throughout the water column, its effective depth range still depends on the background stratification (Teruzzi, et al, 2014; Cossarini et al., 2019; Berthet et al., 2023). The joint assimilation configuration in CHL_SST is therefore not merely a merger of data streams, but a thermodynamically consistent framework that preserves the dynamical expression of biological renewal as the mixed layer deepens or shoals seasonally. For example, at station BY15, CHL_SST brought the SCM depth closer to the observed pycnocline during the 2018 winter transition (Fig. 8), indicating a more realistic coupling between surface forcing and subsurface biomass structure. This spatial correction helps align the simulated biological productive center with the observed nutricline and pycnocline (Teruzzi, et al, 2021), thereby providing a more reliable basis for interpreting subsurface primary production and its potential implications for carbon export.

SST constraints do not only modify the thermal field but also determine the effective vertical extent of biogeochemical corrections (Goodliff et al, 2019). In summer, when the euphotic layer and the seasonal pycnocline are closely aligned, surface biological changes are more readily reflected in the subsurface chlorophyll structure (Barbieux et al., 2019; Baldry et al, 2020; Xu et al, 2022). This limitation is particularly pronounced during the autumn transition. As wind-driven turbulence and convective cooling accelerate the downward entrainment of the mixed layer, the fixed correlation scales within CHL_3D

https://doi.org/10.5194/egusphere-2026-3657
Preprint. Discussion started: 27 July 2026

fail to track the descending pycnocline between 30 and 55 meters. This phenomenon suggests that the failure of purely biological assimilation is not a problem in the observation geometry, but rather a structural conflict between stationary correlation length scales and nonlinear ocean mixing. The primary advantage of integrating SST lies precisely in its ability to dynamically re-adjust this hydrodynamic boundary. In this dynamic context, our results show that biogeochemical corrections affect the SCM only when the hydrographic environment retains sufficient vertical coherence to allow surface anomalies to penetrate below the mixed layer (Kahru et al., 2012; Quartly et al., 2023). The added value of SST lies in its restoration of a physically plausible upper-ocean background, which helps maintain vertical consistency in chlorophyll-related light attenuation, nutrient depletion, and biomass redistribution (Zhang et al., 2016; Sein et al., 2022). SST therefore defines the stratified domain within which biogeochemical signals can be expressed, but it does not directly generate those signals (Behrenfeld et al., 2006).

5.3 Dynamical Decoupling of the Deep Redox Environment

The nearly invariant oxycline trajectories in our results (Fig. 11) reveal that the static benthic boundary layers in the model effectively seal the sediment-water interface, completely insulating deep-water redox renewals from any pelagic biological updates. The weak response of deep oxygen to all assimilation configurations indicates that the deep redox environment is dynamically decoupled from surface biomass (Park et al, 2018; Teruzzi et al., 2021). Below the pycnocline, the oxygen variability is primarily governed by ventilation, basin-scale exchange (Brandt et al. 2015), benthic oxygen demand, and the persistence of the halocline (Kuliński et al., 2022; Kõuts et al., 2021), rather than by surface chlorophyll adjustments. This indicates that deep basins respond to a different controlling regime than the photosynthetic layer, and that the linkage between surface productivity and deep redox state is interrupted by the strong haline stratification in the Baltic Sea.

Improving the upper-ocean biological state does influence oxygen levels in the oxic surface and intermediate layers, but this influence does not extend into the deep basins, where the oxycline remains largely unchanged (Fig. 11). This localized efficacy demonstrates that deep oxygen is therefore not a delayed or smoothed continuation of surface biogeochemical change. Instead, it behaves as a semi-isolated compartment whose state depends on episodic renewal events and on the integrity of the salinity barrier that regulates vertical exchange. This process-level separation explains why forcing the model with either surface satellites (CHL_SAT) or full vertical bioprofiles (CHL_3D) yields diminishing returns below the halocline. Without correcting the underlying physical baseline of vertical transport, the assimilation system remains blind to the deep anoxic pool. This multi-variable vertical coupling and the corresponding performance of different DA configurations are systematically summarized in Table 2.

This suggests that surface biogeochemical corrections cannot be expected to reorganize the deep redox environment unless they are accompanied by independent changes in ventilation or benthic flux conditions. From this perspective, the remaining deep-oxygen bias should not be interpreted simply as a residual model truncation error of the DA algorithm, but rather as a

https://doi.org/10.5194/egusphere-2026-3657
Preprint. Discussion started: 27 July 2026

physical manifestation of missing deep-water constraints. The Baltic Sea should therefore be viewed as a system of partially connected compartments. The photosynthetic zone forms the upper compartment, where biomass, light, and the local thermal structure interact closely. Conversely, the deep basin operates as a separate domain. Its oxygen state is largely controlled by external renewal events and internal consumption processes.

Tabel 2. Hierarchy of physical–biogeochemical controls across the simulated Baltic Sea domains.

Layer / Variable	Dominant control	Key DA configuration	Primary mechanism
Surface SST	Direct thermodynamic forcing	CHL_SST	Kalman update of temperature field
Surface Chl-a (spring)	Thermal stratification & MLD	CHL_SST	Restored physical background optimizes bloom phenology
Surface Chl-a (summer)	Nutrient availability & biomass	CHL_SAT / CHL_3D	Direct state correction of phytoplankton biomass
Subsurface Chl-a / SCM	Thermocline depth & stratification	CHL_3D / CHL_SST	Profile constraints align simulated SCM with the dynamic pycnocline
Bio-optical K_d feedback	Phytoplankton absorption & shading	CHL_SAT	Altered optical attenuation induces vertical heat redistribution
Deep-water redox status	Physical transport & benthic flux	All configurations (no basin-wide improvement)	Dominated by episodic saltwater inflows and sediment remineralization

6 Conclusions

In this study, a weakly coupled data assimilation framework was developed and evaluated for the Baltic Sea that jointly integrates satellite and in situ Chl-a together with SST into the coupled physical–biogeochemical model. The system substantially improves the representation of surface phytoplankton biomass while providing a dynamically consistent view of how bio-optical corrections influence thermal structure and oxygen distributions in a salinity-stratified marginal sea.

First, the experiments demonstrate that Chl-a assimilation markedly enhances the spatial and seasonal structure of surface chlorophyll fields, particularly during seaonsal transition periods and within offshore deep basins where the model strongly underestimates bloom magnitude and incorrectly predicts seasonal phases. Direct SST assimilation is necessary to achieve near-optimal SST skill and, combined with Chl-a constraints, yields the largest and most coherent improvements in regions where physical–biogeochemical coupling is strongest, especially during spring stratification onset. Our results show that

https://doi.org/10.5194/egusphere-2026-3657
Preprint. Discussion started: 27 July 2026

physical and biological observational constraints are complementary rather than redundant, acting synergistically to correct both the state and the context of phytoplankton dynamics.

Second, the analysis reveals a clear vertical hierarchy of control. Surface-only satellite Chl-a assimilation is insufficient to reconstruct the SCM in the stratified central basins, and may even degrade mixed-layer structure if vertical localization is relied upon as the sole pathway for downward influence. Assimilation of in situ Chl-a profiles is essential to constrain the pycnocline-layer biomass and SCM depth (Figs. 7 and 8), while SST assimilation indirectly improves subsurface structure by correcting the seasonal pycnocline and mixed-layer depth. In contrast, the deep-water oxycline remains largely insensitive to any of the tested configurations, confirming that deep oxygen dynamics are dominated by physical ventilation and remineralization processes that lie outside the reach of surface-focused weakly coupled assimilation.

Third, the results demonstrate structural limitations imposed by the optically complex nature of the Baltic Sea. High CDOM concentrations and heterogeneous particulate loads generate substantial uncertainty in satellite Chl-a retrievals, particularly from high-resolution products such as Sentinel-3, which cannot be fully mitigated by statistical error inflation (Fig. 5). In this context, the joint assimilation of Chl-a and SST acts as a form of cross-variable regularization. The physical constraint prevents noisy biological updates from driving the thermal state away from observations, while the biological constraint refines the bio-optical control on vertical heat redistribution within the euphotic zone. These findings are relevant for other CDOM-rich coastal and marginal seas where satellite-based biogeochemical assimilation is pursued under similarly challenging optical conditions.

Finally, the study emphasizes the need to move toward multivariate biogeochemical assimilation if the system is to be used for robust nutrient budget assessment or eutrophication management. Updating only phytoplankton biomass leaves nutrient and detrital pools to adjust solely through model-internal NPZ dynamics, which may be adequate at the basin scale but does not guarantee local stoichiometric consistency. Future developments should therefore prioritize the simultaneous adjustment of nutrients and particulate organic matter in proportion to biomass increments, as well as the inclusion of additional observational constraints such as CDOM or benthic oxygen. In combination with flow–dependent background error covariances, such enhancements would extend the present framework from a process-oriented diagnostic tool toward a more comprehensive operational system for monitoring and forecasting biogeochemical conditions in the Baltic Sea and other optically complex marginal seas.

These results have direct implications for biogeochemical monitoring and eutrophication management in optically complex marginal seas. The 30–39% reduction in Chl-a RMSE improves the reliability of bloom detection and supports more robust eutrophication assessments (e.g., HELCOM indicators) by providing a baseline that better separates anthropogenic nutrient forcing from natural variability. At the same time, surface Chl-a alone cannot constrain deep oxygen dynamics or diagnose

https://doi.org/10.5194/egusphere-2026-3657
Preprint. Discussion started: 27 July 2026

deep hypoxia in the Baltic Sea. Effective eutrophication control requires explicitly accounting for physical ventilation (e.g., Major Baltic Inflows) and benthic processes in addition to biological constraints.

Code and data availability

The NEMO–SCOBI code as applied in this study is available from the SMHI GitLab repository upon registration and login: https://git.smhi.se/fouo/nemo3.6/. The data assimilation code is based on Liu and Fu (2018) and was extended to assimilate chlorophyll-a. The river forcing used in this study is described in Ruvalcaba Baroni et al. (2024) and is freely available therein. The quality-controlled databases used in the present paper are publicly available from CMEMS and OSI SAF. The simulation output is too large to be archived in a public repository; therefore, the data supporting the findings of this study are available from the corresponding author upon reasonable request. Selected output fields and analysis scripts will be deposited in a public repository or provided upon reasonable request.

Author contributions

YL performed the simulations, model output analysis, writing the first draft, and produced the figures. Both YL and WWF participated in the analysis and discussions of the results, and editing of the manuscript.

Competing interests

The authors declare that they have no conflict of interest.

Acknowledgements

The authors are grateful to the Swedish National Supercomputer Centre's High-Performance Computing (HPC) system, which facilitated model simulation and analysis. The Python code used to generate figures in this manuscript and grammar editing with the help of Perplexity.

Financial support

This study was funded by the Swedish Agency for Marine and Water Management (HaVs- och vattenmyndigheten; HaVs) within “Spring oxygen and chlorophyll-a indicators in the Baltic Sea” and Natural Science Foundation of Shanghai under the grant number 24ZR1404500.

https://doi.org/10.5194/egusphere-2026-3657
Preprint. Discussion started: 27 July 2026

Review statement

The review statement will be added by Copernicus Publications listing the handling editor as well as all contributing referees according to their status anonymous or identified.

References

Andersen, J. H., Carstensen, J., Conley, D. J., Dromph, K., Fleming-Lehtinen, V., Gustafsson, B. G., Josefson, A. B., Norkko, A., Villnäs, A., and Murray, C.: Long-term temporal and spatial trends in eutrophication status of the Baltic Sea, Estuar. Coast. Shelf Sci., 198, 102–118, 2017.

Arheimer, B., Dahné, J., Donnelly, C., Lindström, G., and Strömqvist, J.: Water and nutrient simulations using the HYPE model for Sweden vs. the Baltic Sea basin – influence of input-data quality and scale, Hydrol. Res., 43, 315–329, https://doi.org/10.2166/nh.2012.010, 2012.

Balmaseda, M. A., Mogensen, K., and Weaver, A. T.: Evaluation of the ECMWF ocean reanalysis system ORAS4, Q. J. R. Meteorol. Soc., 139, 1132–1161, https://doi.org/10.1002/qj.2063, 2013.

Baldry, K., Strutton, P. G., Hill, N. A., and Boyd, P. W. : Subsurface Chlorophyll-a Maxima in the Southern Ocean, Front. Mar. Sci., 7, 671, https://doi.org/10.3389/fmars.2020.00671, 2020.

Barbieux, M., Uitz, J., Gentili, B., Pasqueron de Fommervault, O., Mignot, A., Poteau, A., Schmechtig, C., Taillandier, V., Leymarie, E., Penkerc'h, C., D'Ortenzio, F., Claustre, H., and Bricaud, A.: Bio-optical characterization of subsurface chlorophyll maxima in the Mediterranean Sea from a Biogeochemical-Argo float database, Biogeosciences, 16, 1321–1342, https://doi.org/10.5194/bg-16-1321-2019, 2019.

Berthet, S., Jouanno, J., Séférian, R., Gehlen, M., and Llovel, W.: How does the phytoplankton–light feedback affect the marine N2O inventory?, Earth Syst. Dynam., 14, 399–412, https://doi.org/10.5194/esd-14-399-2023, 2023.

Behrenfeld, M. J., O'Malley, R. T., Siegel, D. A., McClain, C. R., Sarmiento, J. L., Feldman, G. C., Milligan, A. J., Falkowski, P.G., Letelier, R.M, and Boss, E. S.: Climate-driven trends in contemporary ocean productivity, Nature, 444, 752–755，https://doi.org/10.1038/nature05317, 2006.

Brando, V. E., Sammartino, M., Colella, S., Bracaglia, M., Di Cicco, A., D'Alimonte, D., Kajiyama, T., Kaitala, S., and Attila, J.: Phytoplankton bloom dynamics in the Baltic Sea using a consistently reprocessed time series of multi-sensor reflectance and novel chlorophyll-a retrievals, Remote Sens., 13, 3071, https://doi.org/10.3390/rs13163071, 2021.

Brandt, P., Bange, H. W., Banyte, D., Dengler, M., Didwischus, S.-H., Fischer, T., Greatbatch, R. J., Hahn, J., Kanzow, T., Karstensen, J., Körtzinger, A., Krahmann, G., Schmidtko, S., Stramma, L., Tanhua, T., and Visbeck, M.: On the role of circulation and mixing in the ventilation of oxygen minimum zones with a focus on the eastern tropical North Atlantic, Biogeosciences, 12(2), 489–512, https://doi.org/10.5194/bg-12-489-2015, 2015.

https://doi.org/10.5194/egusphere-2026-3657
Preprint. Discussion started: 27 July 2026

Cahill, B. E., Kowalczuk, P., Kritten, L., Gräwe, U., Wilkin, J., and Fischer, J.: Estimating the seasonal impact of optically significant water constituents on surface heating rates in the western Baltic Sea, Biogeosciences, 20, 2743–2768, https://doi.org/10.5194/bg-20-2743-2023, 2023.

Carrassi, A., Bocquet, M., Bertino, L., and Evensen, G.: Data assimilation in the geosciences: an overview of methods, issues, and perspectives, WIREs Clim. Change, 9, e535, https://doi.org/10.1002/wcc.535, 2018.

Carstensen, J., Conley, D. J., Almroth-Rosell, E., Asmala, E., Bonsdorff, E., Fleming-Lehtinen, V., Gustafsson, B. G., Gustafsson, C., Heiskanen, A.-S., Janas, U., Norkko, A., Slomp, C. P., Villnäs, A., Voss, M., and Zilius, M.: Factors regulating the coastal nutrient filter in the Baltic Sea, Ambio, 49, 1194–1210, 2020.

Ciavatta, S., Brewin, R. J. W., Skákala, J., Polimene, L., de Mora, L., Artioli, Y., and Allen, J. I.: Assimilation of ocean-color plankton functional types to improve marine ecosystem simulations, J. Geophys. Res. Oceans, 123, 834–854, https://doi.org/10.1002/2017JC013490, 2018.

Clow, G. L., Lovenduski, N. S., Levy, M. N., Lindsay, K., Mogen, S. C., and Kay, J. E.: Detectability of phytoplankton biomass extremes using simulated satellite chlorophyll observations, Geophys. Res. Lett., 53, e2025GL121347, https://doi.org/10.1029/2025GL121347, 2026.

Copernicus Climate Change Service, Climate Data Store: Complete UERRA regional reanalysis for Europe from 1961 to 2019. Copernicus Climate Change Service (C3S) Climate Data Store (CDS). DOI: 10.24381/cds.dd7c6d66 (Accessed on 19 June 2026), 2019

Davies, H. C.: A lateral boundary formulation for multi-level prediction models, Q. J. R. Meteorol. Soc., 102, 405–418, 1976.

Donlon, C. J., Martin, M., Stark, J., Roberts-Jones, J., Fiedler, E., and Wimmer, W.: The Operational Sea Surface Temperature and Sea Ice Analysis (OSTIA) system, Remote Sens. Environ., 116, 140–158, https://doi.org/10.1016/j.rse.2010.10.017, 2012.

Eilola, K., Meier, H. E. M., and Almroth, E.: On the dynamics of oxygen, phosphorus and cyanobacteria in the Baltic Sea: a model study, J. Mar. Syst., 75, 163–184, 2009.

Flather, R. A.: A storm surge prediction model for the northern Bay of Bengal with application to the cyclone disaster in April 1991, J. Phys. Oceanogr., 24, 172–190, 1994.

Fonselius, S. H.: Hydrography of the Baltic deep basins, Fiskeristyrelsen, available at: https://www.diva-portal.org/smash (last access: January 2024), 1962.

Ford, D., and Barciela, R.: Global marine biogeochemical reanalyses assimilating two different sets of merged ocean colour products, Remote Sens. Environ., 203, 40–54, https://doi.org/10.1016/j.rse.2017.03.040, 2017.

Galperin, B., Kantha, L. H., Hassid, S., and Rosati, A.: A quasi-equilibrium turbulent energy model for geophysical flows, J. Atmos. Sci., 45, 55–62, 1988.

Gentemann, C. L., Minnett, P. J., and Ward, B.: Profiles of ocean surface heating (POSH): a new model of upper ocean diurnal warming, J. Geophys. Res. Oceans, 114, C07017, https://doi.org/10.1029/2008JC004825, 2009.

https://doi.org/10.5194/egusphere-2026-3657
Preprint. Discussion started: 27 July 2026

Gnanadesikan, A., and Anderson, W. G.: Ocean water clarity and the ocean general circulation in a coupled climate model, J. Phys. Oceanogr., 39, 314–332, 2009.

Goodliff, M., Bruening, T., Schwichtenberg, F., Li, X., Lindenthal, A., Lorkowski, I., and Nerger, L.: Temperature assimilation into a coastal ocean-biogeochemical model: assessment of weakly and strongly coupled data assimilation, Ocean Dyn., 69, 1217–1237, 2019.

Cossarini, G., Mariotti, L., Feudale, L., Mignot, A., Salon, S., Taillandier, V., Teruzzi, A., and D'Ortenzio, F.: Towards operational 3D-Var assimilation of chlorophyll Biogeochemical-Argo float data into a biogeochemical model of the Mediterranean Sea, Ocean Model., 133, 112-128, 2019.

Gustafsson, B. G., Schenk, F., Blenckner, T., Eilola, K., Meier, H. E. M., Müller-Karulis, B., Neumann, T., Ruoho-Airola, T., Savchuk, O.P., and Zorita, E. : Reconstructing the development of Baltic Sea eutrophication 1850–2006, Ambio, 41, 534–548, https://doi.org/10.1007/s13280-012-0318-x, 2012.

Jahanmard, V., Ellmann, A., and Delpeche-Ellmann, N.: Quantification of Baltic Sea water budget components using dynamic topography, Ocean Sci., 21, 913–930, https://doi.org/10.5194/os-21-913-2025, 2025.

Kahru, M., Kudela, R. M., Manzano-Sarabia, M., and Mitchell, B. G.: Trends in the surface chlorophyll of the California Current: Merging MODIS and SeaWiFS data, Deep-Sea Res. II: Top. Stud. Oceanogr., 57(21-22), 89–98, https://doi.org/10.1016/j.dsr2.2012.04.007, 2012.

Kang, E.-J., Sohn, B.-J., Kim, S.-W., Kim, W., Kwon, Y.-C., Kim, S.-B., Chun, H.-W., and Liu, C.: A revised ocean mixed layer model for better simulating the diurnal variation in ocean skin temperature, Geosci. Model Dev., 17, 8553–8568, https://doi.org/10.5194/gmd-17-8553-2024, 2024.

Karspeck, A. R., Danabasoglu, G., Anderson, J., Karol, S., Collins, N., Vertenstein, M., Raeder, K., Hoar, T., Neale, R., Edwards, J., and Craig, A.: A global coupled ensemble data assimilation system using the community earth system model and the data assimilation research testbed, Q. J. R. Meteorol. Soc., 144, 2404–2430, https://doi.org/10.1002/qj.3308, 2018.

Klais, R., Lehtinen, S., Tamminen, T., and Tamminen, T.: Seasonal and spatial changes of primary production in the Baltic Sea based on 26 years of in situ 14C measurements, Front. Mar. Sci., 7, 604532, https://doi.org/10.3389/fmars.2020.604532, 2021.

Kratzer, S., and Moore, G.: Inherent optical properties of Baltic Sea waters and implications for satellite retrievals, Remote Sens. Environ., 217, 13–27, 2018.

Kuliński, K., Rehder, G., Asmala, E., Bartosova, A., Carstensen, J., Gustafsson, B., Hall, P. O. J., Humborg, C., Jilbert, T., Jürgens, K., Meier, H. E. M., Müller-Karulis, B., Naumann, M., Olesen, J. E., Savchuk, O., Schramm, A., Slomp, C. P., Sofiev, M., Sobek, A., Szymczycha, B., and Undeman, E.: Biogeochemical functioning of the Baltic Sea, Earth Syst. Dynam., 13, 633–685, https://doi.org/10.5194/esd-13-633-2022, 2022.

Kõuts, M., Maljutenko, I., Elken, J., Liu, Y., Hansson, M., Viktorsson, L., and Raudsepp, U.: Recent regime of persistent hypoxia in the Baltic Sea, Environ. Res. Commun., 3(7), 075004, https://doi.org/10.1088/2515-7620/ac0cc4., 2021.

https://doi.org/10.5194/egusphere-2026-3657
Preprint. Discussion started: 27 July 2026

Lai, W., Gan, J., Liu, Y., Liu, Z., Xie, J., and Zhu, J.: Assimilating in situ and remote sensing observations in a highly variable estuary–shelf model, J. Atmos. Ocean. Technol., 38, 459–479, https://doi.org/10.1175/JTECH-D-20-0084.1, 2021.

Lavigne, H., Van der Zande, D., Ruddick, K., Cardoso Dos Santos, J. F., Gohin, F., Brotas, V., and Kratzer, S.: Quality-control tests for OC chlorophyll algorithms in coastal waters, Remote Sens. Environ., 255, 112246, https://doi.org/10.1016/j.rse.2020.112237, 2021.

Leclair, M., and Madec, G.: A conservative leapfrog time stepping method, Ocean Model., 30, 88–94, https://doi.org/10.1016/j.ocemod.2009.06.006, 2009.

Lengaigne, M., Menkes, C., Aumont, O., Gorgues, T., Bopp, L., André, J.-M., and Madec, G.: Influence of the oceanic biology on the tropical Pacific climate in a coupled general circulation model, Clim. Dynam., 28, 503–516, https://doi.org/10.1007/s00382-006-0200-2, 2007.

Lévy, M., Klein, P., and Tréguier, A.-M.: Impact of sub-mesoscale physics on production and subduction of phytoplankton in an oligotrophic regime, J. Mar. Res., 59, 535–565, 2001.

Liblik, T., Väli, G., Salm, K., Laanemets, J., Lilover, M.-J., and Lips, U.: Quasi-steady circulation regimes in the Baltic Sea, Ocean Sci., 18, 857–879, https://doi.org/10.5194/os-18-857-2022, 2022.

Liu, Y., and Fu, W. W.: Assimilating high-resolution sea surface temperature data improves the ocean forecast potential in the Baltic Sea, Ocean Sci., 14, 525–541, 2018.

Liu, Y., Meier, H. E. M, and Eilola, E.: Improving the multiannual, high-resolution modelling of biogeochemical cycles in the Baltic Sea by using data assimilation, Tellus A: Dyn. Meteorol. Oceanogr., 66(1). https://doi.org/10.3402/tellusa.v66.24908, 2014.

Liu, Y., Meier, H. E. M., and Axell, L.: Reanalyzing temperature and salinity on decadal time scales using the ensemble optimal interpolation data assimilation method and a 3-D ocean circulation model of the Baltic Sea, J. Geophys. Res. Oceans, 118, 5536–5554, 2013.

Liu, Y., Xie, J., Liu, Z., Gan, J., and Zhu, J.: The assimilation of temperature and salinity profile observations for forecasting the river–estuary–shelf waters, J. Geophys. Res. Oceans, 126 (10), e2020JC017043, https://doi.org/10.1029/2020JC017043, 2021.

Löptien, U., and Meier, H. E. M.: The influence of increasing water turbidity on the sea surface temperature in the Baltic sea: A model sensitivity study, J. Marine Syst., 88, 323–331, https://doi.org/10.1016/J.JMARSYS.2011.06.001, 2011.

Löptien, U., Eden, C., Timmermann, A., and Dietze, H.: Effects of biologically induced differential heating in an eddy-permitting coupled ocean-ecosystem model, J. Geophys. Res., 114, C06011, https://doi.org/10.1029/2008JC004936, 2009.

Manizza, M., Le Quéré, C., Watson, A. J., and Buitenhuis, E. T.: Bio-optical feedbacks among phytoplankton, upper ocean physics and sea-ice in a global model, Geophys. Res. Lett., 32, L05603, https://doi.org/10.1029/2004GL020778, 2005.

Maúre, E. d. R., Terauchi, G., Ishizaka, J., Clinton, N., and DeWitt., M. : Globally consistent assessment of coastal eutrophication, Nat. Commun., 12, 6142, https://doi.org/10.1038/s41467-021-26391-9, 2021.

https://doi.org/10.5194/egusphere-2026-3657
Preprint. Discussion started: 27 July 2026

Meier, H. E. M., Edman, M. K., Eilola, K. J., Placke, M., Neumann, T., Andersson, H. C., Radtke, H., Saraiva, S., and Wåhlström, I. : Future projections of record-breaking sea surface temperature and cyanobacteria bloom events in the Baltic Sea, Ambio, 48, 1362–1376, https://doi.org/10.1007/s13280-019-01235-5, 2019.

Meier, H. E. M., Kniebusch, M., Dieterich, C., Gröger, M., Zorita, E., Elmgren, R., Myrberg, K., Ahola, M. P., Bartosova, A., Bonsdorff, E., Börgel, F., Capell, R., Carlén, I., Carlund, T., Carstensen, J., Christensen, O. B., Dierschke, V., Frauen, C., Frederiksen, M., Gaget, E., Galatius, A., Haapala, J. J., Halkka, A., Hugelius, G., Hünicke, B., Jaagus, J., Jüssi, M., Käyhkö, J., Kirchner, N., Kjellström, E., Kulinski, K., Lehmann, A., Lindström, G., May, W., Miller, P. A., Mohrholz, V., Müller-Karulis, B., Pavón-Jordán, D., Quante, M., Reckermann, M., Rutgersson, A., Savchuk, O. P., Stendel, M., Tuomi, L., Viitasalo, M., Weisse, R., and Zhang, W.: Climate change in the Baltic Sea region: a summary, Earth Syst. Dynam., 13, 457–593, https://doi.org/10.5194/esd-13-457-2022, 2022.

Meier, H. E. M., Müller-Karulis, B., Andersson, H. C., Dieterich, C., Eilola, K., Gustafsson, B. G., Höglund, A., Hordoir, R., Kuznetsov, I., Neumann, T., Ranjbar, Z., Savchuk, O.P., and Schimanke, S.: Impact of climate change on ecological quality indicators and biogeochemical fluxes in the Baltic Sea: a multi-model ensemble study, Ambio, 41, 558–573, https://doi.org/10.1007/s13280-012-0320-3, 2012.

Meng, S., Webber, B. G. M., Stevens, D. P., Joshi, M., Palmieri, J., and Yool, A.: Diverse responses of upper ocean temperatures to chlorophyll-induced solar absorption across different coastal upwelling regions. Geophys. Res. Lett., 51, e2024GL109714. https://doi. org/10.1029/2024GL109714, 2024.

Merchant, C. J., Paul, F., Popp, T., Ablain, M., Bontemps, S., Defourny, P., Hollmann, R., Lavergne, T., Laeng, A., de Leeuw, G., Mittaz, J., Poulsen, C., Povey, A. C., Reuter, M., Sathyendranath, S., Sandven, S., Sofieva, V., and Wagner, W.: Version 2 of the EUMETSAT OSI SAF and ESA CCI sea-ice concentration climate data records, Cryosphere, 13, 49–77, https://doi.org/10.5194/tc-13-49-2019, 2019.

Mohrholz, V.: Major Baltic inflow statistics – revised, Front. Mar. Sci., 5, 384, https://doi.org/10.3389/fmars.2018.00384, 2018.

Neumann, T., Koponen, S., Attila, J., Brockmann, C., Kallio, K., Kervinen, M., Mazeran, C., Müller, D., Philipson, P., Thulin, S., Väkevä, S., and Ylöstalo, P.: Optical model for the Baltic Sea with an explicit CDOM state variable: a case study with Model ERGOM (version 1.2), Geosci. Model Dev., 14, 5049–5062, https://doi.org/10.5194/gmd-14-5049-2021, 2021.

Park, J.-Y., Kug, J.-S., Seo, H., and Bader, J.: Impact of bio-physical feedbacks on the tropical climate in coupled and uncoupled GCMs, Clim. Dynam., 43, 1811–1827, https://doi.org/10.1007/s00382-013-2009-0, 2014.

Park, J.-Y., Stock, C. A., Yang, X., Dunne, J. P., Rosati, A., John, J., and Zhang, S.: Modeling Global Ocean Biogeochemistry With Physical Data Assimilation: A Pragmatic Solution to the Equatorial Instability, J. Adv. Model. Earth Syst., 10(4), 891–906, https://doi.org/10.1002/2017ms001223, 2018.

Quartly, G. D., Aiken, J., Brewin, R. J. W., and Yool, A.: The link between surface and sub-surface chlorophyll-a in the centre of the Atlantic subtropical gyres: a comparison of observations and models, Front. Mar. Sci., 10, 1197753, doi: 10.3389/fmars.2023.1197753, 2023.

https://doi.org/10.5194/egusphere-2026-3657
Preprint. Discussion started: 27 July 2026

Ridal, M., Olsson, E., Unden, P., Zimmermann, K., Ohlsson, A.: Uncertainties in Ensembles of Regional Re-Analyses. Deliverable D2.7 HARMONIE Reanalysis Report of Results and Dataset. available at https://www.uerra.eu, last access: June 2026, 2017.

Ruvalcaba Baroni, I., Almroth-Rosell, E., Axell, L., Fredriksson, S. T., Hieronymus, J., Hieronymus, M., Brunnabend, S.-E., Gröger, M., Kuznetsov, I., Fransner, F., Hordoir, R., Falahat, S., and Arneborg, L.: Validation of the coupled physical–biogeochemical ocean model NEMO–SCOBI for the North Sea–Baltic Sea system, Biogeosciences, 21, 2087–2132, https://doi.org/10.5194/bg-21-2087-2024, 2024.

Savchuk, O. P. (2018). Large-scale nutrient dynamics in the Baltic Sea, 1970–2016. Front. Mar. Sci., 5, 95. https://doi.org/10.3389/fmars.2018.00095, 2018.

Sein, D. V., Dvornikov, A. Y., Martyanov, S. D., Cabos, W., Ryabchenko, V. A., Gröger, M., Jacob, D., Kumar Mishra, A., and Kumar, P.: Indian Ocean marine biogeochemical variability and its feedback on simulated South Asia climate, Earth Syst. Dynam., 13, 809–831, https://doi.org/10.5194/esd-13-809-2022, 2022

She J., Berg, P., and Berg, J.: Bathymetry impacts on water exchange modelling through the Danish Straits, J. Mar. Syst., 65, 450-459, https://doi.org/10.1016/j.jmarsys.2006.01.017, 2007.

Siegel, D.A., Behrenfeld, M.J., Maritorena, S., McClain, C. R., Antoine, D., Bailey, S.W., Bontempi, P.S.,Boss, E.S, Dierssen, H.M., Doney, S.C., Eplee Jr., R.E., Evans, R.H., Feldman, G.C., Fields, E., Franz, B.A., Kuring, N.A., Mengelt, C., Nelson, N.B., Patt, F.S., Robinson, W.D., Sarmiento, J.L., Swan, C.M., Werdell, P.J., Westberry, T.K., Wilding, J.G., and Yoder, J.A.: Regional to global assessments of phytoplankton dynamics from the SeaWIFS mission. Remote Sens. Environ., 135, 77–91. https://doi.org/10.1016/j.rse.2013.03.025, 2013.

Simis, S. G. H., Ylöstalo, P., Kallio, K. Y., Spilling, K., and Tiit Kutser, T.: Contrasting seasonality in optical–biogeochemical properties of the Baltic Sea. J. Geophys. Res. Oceans, 122, 6913–6930, 2017

Soomets, T., Toming, K., Paavel, B., and Kutser, T.: Evaluation of remote sensing and modeled chlorophyll-a products of the Baltic Sea, J. Appl. Remote Sens., 16 (4), 046516, https://doi.org/10.1117/1.JRS.16.046516, 2022

Stammer, D., Balmaseda, M., Heimbach, P., Köhl, A., and Weaver, A.: Ocean data assimilation in support of climate applications: status and perspectives. Ann Rev Mar Sci., 8(1): 491–518. doi:10.1146/annurev-marine-122414-034113, 2016.

Stramska, M., and Jakacki, J.: Variability of chlorophyll a concentration in surface waters of the open Baltic Sea,Oceanologia, 66(2), 365-380, 10.1016/j.oceano.2024.02.003, 2024.

Skákala, J., Ford, D., Bruggeman, J., Hull, T., Kaiser, J., King, R. R, Loveday, B., Palmer, M., R., Smyth, T., Williams, C. A. J., and Ciavatta, S.: Towards a multi-platform assimilative system for the North Sea: weakly coupled physical–biogeochemical data assimilation. J. Geophys. Res. Oceans, 126, e2020JC016649, https://doi.org/10.1029/2020JC016649, 2021.

Teruzzi, A, Dobricic, S., Solidoro, C., and Cossarini, G.: A 3-D variational assimilation scheme in coupled transport-biogeochemical models: forecast of Mediterranean biogeochemical properties, J. Geophys. Res. Oceans, 119, 200-217, https://doi.org/10.1002/2013JC009277, 2014.

https://doi.org/10.5194/egusphere-2026-3657
Preprint. Discussion started: 27 July 2026

Teruzzi, A., Bolzon, G., Feudale, L., and Cossarini, G.: Deep chlorophyll maximum and nutricline in the Mediterranean Sea: emerging properties from a multi-platform assimilated biogeochemical model experiment, Biogeosciences, 18, 6147–6166, https://doi.org/10.5194/bg-18-6147-2021, 2021.

Tilstone, G. H., Pardo, S., Simis, S. G. H., Qin, P., Selmes, N., Dessailly, D., and Kwiatkowska, E.: Consistency between Satellite Ocean Colour Products under High Coloured Dissolved Organic Matter Absorption in the Baltic Sea, Remote Sens. 14(1), 89; https://doi.org/10.3390/rs14010089, 2022.

Umlauf, L., and Burchard, H.: A generic length-scale equation for geophysical turbulence models. J. Marine Syst. 61, 235-265, 2003.

Viljoen, J.J., Sun, X., and Brewin, R.J.W. : Climate variability shifts the vertical structure of phytoplankton in the Sargasso Sea, Nat. Clim. Change, 14, 1292–1298, https://doi.org/10.1038/s41558-024-02136-6, 2024.

von Schuckmann, K., Le Traon, P.-Y., Smith, N., Pascual, A., Djavidnia, S., Gattuso, J.-P., Grégoire, M., Aaboe, S., Alari, V., Alexander, B. E., Alonso-Martirena, A., Aydogdu, A., Azzopardi, J., Bajo, M., Barbariol, F., Batistić, M., Behrens, A., Ben Ismail, S., Benetazzo, A., Bitetto, I., Borghini, M., Bray, L., Capet, A., Carlucci, R., Chatterjee, S., Chiggiato, J., Ciliberti, S., Cipriano, G., Clementi, E., Cochrane, P., Cossarini, G., D'Andrea, L., Davison, S., Down, E., Drago, A., Druon, J.-N., Engelhard, G., Federico, I., Garić, R., Gauci, A., Gerin, R., Geyer, G., Giesen, R., Good, S., Graham, R., Grégoire, M., Greiner, E., Gundersen, K., Hélaouët, P., Hendricks, S., Heymans, J. J., Holt, J., Hure, M., Juza, M., Kassis, D., Kellett, P., Knol-Kauffman, M., Kountouris, P., Kõuts, M., Lagemaa, P., Lavergne, T., Legeais, J.-F., Le Traon, P.-Y., Libralato, S., Lien, V. S., Lima, L., Lind, S., Liu, Y., Macías, D., Maljutenko, I., Mangin, A., Männik, A., Marinova, V., Martellucci, R., Masnadi, F., Mauri, E., Mayer, M., Menna, M., Meulders, C., Møgster, J. S., Monier, M., Mork, K. A., Müller, M., Øie Nilsen, J. E., Notarstefano, G., Oviedo, J. L., Palerme, C., Palialexis, A., Panzeri, D., Pardo, S., Peneva, E., Pezzutto, P., Pirro, A., Platt, T., Poulain, P.-M., Prieto, L., Querin, S., Rabenstein, L., Raj, R. P., Raudsepp, U., Reale, M., Renshaw, R., Ricchi, A., Ricker, R., Rikka, S., Ruiz, J., Russo, T., Sanchez, J., Santoleri, R., Sathyendranath, S., Scarcella, G., Schroeder, K., Sparnocchia, S., Spedicato, M. T., Stanev, E., Staneva, J., Stocker, A., Stoffelen, A., Teruzzi, A., Townhill, B., Uiboupin, R., Valcheva, N., Vandenbulcke, L., Vindenes, H., von Schuckmann, K., Vrgoč, N., Wakelin, S., and Zupa, W.: Copernicus Marine Service Ocean State Report, Issue 5. J. Oper. Oceanogr., 12, 1–123. https://doi.org/10.1080/1755876X.2019.1633075, 2019.

Wang, B., Fennel, K., and Yu, L.: Can assimilation of satellite observations improve subsurface biological properties in a numerical model? A case study for the Gulf of Mexico, Ocean Sci., 17, 1141–1156, https://doi.org/10.5194/os-17-1141-2021, 2021.

Xu, W., Wang, G., Cheng, X., Jiang, L., Zhou, W., and Cao, W.: Characteristics of subsurface chlorophyll maxima during the boreal summer in the South China Sea with respect to environmental properties, Sci. Total Environ., 820, 153243, https://doi.org/10.1016/j.scitotenv.2022.153243, 2022.

Zhang, W.-Z., Wang, H., Chai, F., and Qiu, G.: Physical drivers of chlorophyll variability in the open South China Sea, J. Geophys. Res. Oceans, 121(9), 7123–7140, https://doi.org/10.1002/2016JC011983, 2016.

https://doi.org/10.5194/egusphere-2026-3657
Preprint. Discussion started: 27 July 2026

Zuo, H., Balmaseda, M. A., Mogensen, K., and Tietsche, S.: OCEAN5: The ECMWF Ocean reanalysis system and its real-time analysis component, ECMWF Tech Memorandum, 44, https://doi.org/10.21957/la2v0442, 2018.